

## COMPOSITE $M_v$ VERSUS $(V-I)_0$ DIAGRAM FOR TEMPLATE OPEN CLUSTERS

ANDRÉS E. PIATTI<sup>1</sup> AND JUAN J. CLARÍA

Observatorio Astronómico, Laprida 854, 5000, Córdoba, Argentina; andres@oac.uncor.edu, claria@oac.uncor.edu

AND

EDUARDO BICA

Universidade Federal do Rio Grande do Sul, Departamento de Astronomia, CP 15051, Porto Alegre, 91500-970, Brazil; bica@if.ufrgs.br

Received 1997 August 20; accepted 1998 January 7

### ABSTRACT

New CCD  $VI$  photometric data for 10 template open clusters with accurately determined fundamental parameters are presented. From the observed  $V$  versus  $V-I$  diagrams of the clusters, fiducial sequences have been defined and transformed into the  $M_v$  versus  $(V-I)_0$  diagram by averaging sequences of template open clusters with similar ages. The resulting composite  $M_v$  versus  $(V-I)_0$  diagram presents a homogeneous set of empirical isochrones in the age range between 5 Myr and 4 Gyr. These empirical isochrones show an overall very good agreement with those computed from stellar evolutionary models. Theoretical isochrones with moderate overshooting fit the observed main sequences better than the canonical ones for clusters older than 600 Myr. The present set of empirical isochrones will be useful for the study of faint reddened open clusters

*Subject headings:* open clusters and associations: general — Hertzsprung-Russell diagram — stars: evolution

### 1. INTRODUCTION

The study of Galactic open clusters is of great interest in several astrophysical aspects. Young open clusters provide information about current star formation processes and are key objects for clarifying questions of galactic structure, while old and intermediate-age open clusters play an important role in linking the theories of stellar and galactic evolution. During the last few years, a considerable amount of high-quality photometric and spectroscopic data on open clusters has been collected. Consequently, a statistically significant sample of relatively well studied open clusters is presently available. In fact, several open clusters observed with photographic and/or photoelectric techniques have been reobserved with CCD detectors, and their fundamental parameters have been improved (see, e.g., Montgomery, Marschall, & Janes 1993; Daniel et al. 1994). On the other hand, poorly studied open clusters or those with unknown basic parameters have also been recently observed via CCD photometry (see, e.g., Carraro & Ortolani 1994; Patat & Carraro 1995). We have recently started a program that consists basically of obtaining CCD color-magnitude ( $C-M$ ) and color-color ( $C-C$ ) diagrams of numerous still unstudied objects cataloged as open clusters, mostly located in the direction of the Galactic center. The  $C-M$  and  $C-C$  diagrams of an open cluster are valuable tools for obtaining basic information about the cluster, such as its distance and age, and for studying both interstellar extinction in the direction of the cluster and stellar evolution. The distances, ages, and stellar contents of open clusters give information on the star formation histories, structure, and evolution of the Galaxy. Recent papers (Geisler, Clariá, & Minniti 1992; Friel & Janes 1993; Piatti, Clariá, & Abadi 1995) have fueled the interest for new and independent determinations of physical parameters of open clusters located in the direc-

tion of the Galactic center. The determination of interstellar reddening, distance, and age of an open cluster can be performed by comparing its observed  $C-M$  diagram with those of template open clusters whose basic parameters are accurately known. The most relevant features to take into account in the comparison are the shape and relative positions of the main cluster sequences, the giant clumps, and the morphology of the ascending giant branches, whenever these two latter features exist. As is well known, a large sample of open clusters with a wide age range has already been observed in the  $UBV$  system. Mermilliod (1981a) has constructed  $M_v$  versus  $(B-V)_0$  and  $M_v$  versus  $(U-B)_0$  diagrams by superimposition of several clusters in different age groups. The 14 pairs of composite diagrams established by Mermilliod (1981a) allowed him to determine a homogeneous set of empirical isochrones in both the  $M_v$  versus  $(B-V)_0$  and  $M_v$  versus  $(U-B)_0$  planes for clusters younger than about 600 Myr (Mermilliod 1981b). However, when a cluster is affected by significant reddening—as is the case for objects located toward the Galactic center—the information provided by the  $U,B$  passbands may turn out to be insufficient as the object becomes virtually invisible in these wavelengths. In this case, a  $C-M$  diagram based on information obtained from near-IR passbands, including, for example, the very often used  $I$  filter of the Cousins system, is clearly more useful. Therefore, the calibration of the  $M_v$  versus  $(V-I)_0$  diagram in terms of age through the determination of empirical isochrones equivalent to those drawn by Mermilliod (1981b) in the  $UBV$  system should be very useful in deriving reddening, distance, and age of highly reddened open clusters. Furthermore, the empirical isochrones in the  $M_v$  versus  $(V-I)_0$  plane may also place important constraints on theoretical models of stellar evolution. In this paper empirical isochrones for open clusters in a wide age range have been determined from CCD  $C-M$  diagrams of 10 template open clusters. These isochrones have been placed in a composite diagram that presents the observational results on stellar evolution in the  $M_v$  versus

<sup>1</sup> Visiting Astronomer, University of Toronto (David Dunlap Observatory) 24 Inch Telescope, Las Campanas Observatory, Chile.

$(V-I)_0$  plane. In § 2 we describe the CCD observations of template open clusters and discuss the data reduction procedure. Section 3 deals with the determination of the empirical isochrones. Section 4 is devoted to the comparison of empirical isochrones with those derived from theoretical models. Finally, § 5 summarizes the main results and conclusions of our work.

## 2. OBSERVATIONS AND REDUCTIONS

To determine a homogeneous set of empirical isochrones in the  $M_v$  versus  $(V-I)_0$  plane, observations through the  $V$  and  $I$  bands of open clusters with a wide age range are needed, particularly of those whose fundamental parameters have been accurately determined. During the last few years, several photometric  $VI$  studies of open clusters have been carried out in which observed  $C-M$  diagrams are compared with theoretical isochrones (see, e.g., Mazur, Kaluzny, & Krzemiński 1993; Carraro & Ortolani 1994; Rosvick 1995; Sagar & Cannon 1995). However, a significant sample of known clusters (templates) with a wide age range observed in the  $VI$  Johnson-Cousins system is not presently available. For this reason, we have selected clusters previously studied in detail with comparatively small angular diameters so as to perform CCD observations. Unfortunately, only a minor percentage of the template clusters appears in the sky as relatively concentrated objects. The regions to be observed in the cluster fields were carefully chosen in order to include representative stellar populations of the clusters. In old and intermediate-age clusters, for example, it is important to observe red giants, while in the youngest clusters, the observation of supergiants, if they exist, is fundamental. However, in some comparatively extended clusters or those having few giants in the outer regions, the most concentrated region of the cluster was observed rather than the scarce evolved members located in the outer zones. The selected open clusters cover an important fraction of the timescale over which the Galactic disk evolution has occurred. Table 1 lists the observed sample of template open clusters. As these objects were observed during a run together with unstudied open clusters in the direction of the Galactic center, only clusters clearly separated by age were observed. These template clusters were used as calibrators to derive reddening, distance, and age of the unstudied open clusters. The observations were carried out during a run in 1995 June–July. The direct images were obtained with the 24 inch (61 cm) telescope of

the University of Toronto Southern Observatory at Las Campanas Observatory (Chile). This telescope is equipped with a PM 512 × 512 METACHROME CCD, which has been coated to give improved blue response. The scale on the chip is 0".45 pixel<sup>-1</sup>, and consequently the sky area covered by a single frame is about 4' × 4'. All the cluster fields were observed in two and three different positions which allowed for a slight overlap in most of them. Table 2 summarizes the gathered observational data. Observations of 12 standard stars taken from the lists of Landolt (1983, 1992) were performed nightly. In addition, exposures of bias, sky, and dome flat fields were taken at the beginning and/or at the end of each night to calibrate the chip response. The observations have been reduced using the facilities at the Observatorio Astronómico of the National University of Córdoba (Argentina). In order to clean the images by removing their instrumental signatures, we have applied the averaged bias and flat-field corrections with IRAF standard routines. The averaged twilight and dome flat fields were also used to check possible effects due to nonperpendicularity of the optical path on the chip; no correction was found to be necessary. To obtain instrumental  $v$  and  $i$  magnitudes, we have used the DAOPHOT (Stetson 1991) package in the standard way in the IRAF environment. Aperture photometry of standard stars was performed with an aperture radius equal to 16 pixels (7".2). The relations adopted between the instrumental and standard color and magnitudes are the following:

$$v_{j,n} = v_1 + V + v_2 X_{j,n} + v_3(V-I) \quad (1)$$

$$i_{k,n} = i_1 + I + i_2 X_{k,n} + i_3(V-I), \quad (2)$$

where  $X_j$  and  $X_k$  are air masses corresponding to the frames  $j$  and  $k$ , respectively, and  $V$  and  $(V-I)$  represent the standard magnitude and color. Notice that for each night  $n$  there are as many frames in the different filters as observed standard stars, so that equations (1) and (2) were fitted by least squares simultaneously. Table 3 lists the resulting coefficient values for each night. The mean rms error affecting the calibration in equation (1) is 0.009, while the corresponding one in equation (2) is 0.011, which indicates that the nights were all of excellent photometric quality. The inversion of these expressions allowed us to transform the instrumental colors and magnitudes of the stars measured in the field of the template clusters to the standard  $VI$  Johnson-Cousins system. At this stage, we have obtained four to six independent  $V$ ,  $(V-I)$  table sets for each cluster, together with the  $V$  frame coordinates ( $X$  and  $Y$ ) and the instrumental DAOPHOT.ALLSTARS rms errors. Then, we performed a cross-correlation identification among all  $V$ ,  $(V-I)$  cluster tables averaging  $V$  and  $(V-I)$  values after applying appropriate offsets to the coordinates. The results are improved cluster sets of color and magnitude values as compared to those based on a single measure. Consequently, for stars with more than one measure, possible anomalous values caused by the presence of contamination (e.g., cosmic rays) were minimized. This procedure allowed us also to estimate the photometric internal errors ( $\sigma$ ). Typically  $\sigma(V) \leq 0.02$  mag and  $\sigma(V-I) \leq 0.03$  mag for  $V < 15$  mag, increasing to 0.04 and 0.05 at  $V \approx 18$ , respectively. Tables 4, 5, 6, 7, 8, 9, 10, 11, 12, and 13 present the  $VI$  photometry for 10 template open clusters. Their columns give in succession the star identification number, the coordinates  $X$  and  $Y$  (in pixels), the  $V$  magnitude, the standard

TABLE 1  
SELECTED TEMPLATE OPEN CLUSTERS

Cluster	R.A. (1995.5)	Decl. (1995.5)	Angular Diameter <sup>a</sup> (arcmin)
NGC 3680.....	11 25 28	-43 13 01	11
NGC 3766.....	11 35 56	-61 35 07	10
NGC 6025.....	16 03 17	-60 29 32	12
NGC 6067.....	16 12 53	-54 11 57	15
NGC 6231.....	16 53 42	-41 47 26	15
NGC 6242.....	16 55 20	-39 29 20	9
NGC 6259.....	17 00 24	-44 40 01	12
IC 4651.....	17 24 19	-49 56 28	14
NGC 6451.....	17 50 24	-30 13 00	6
NGC 6633.....	18 27 31	+06 33 45	20

NOTE.—Units of right ascension are hours, minutes, and seconds, and units of declination are degrees, arcminutes, and arcseconds.

<sup>a</sup> Alter, Ruprecht, & Vanýsek 1970.

TABLE 2  
JOURNAL OF OBSERVATIONS

Cluster	Date (UT)	Filter	Exposures (s)	FWHM (arcsec)
NGC 3680 (Center) .....	1995 Jun 30	<i>V</i>	2 × 30	1.6
		<i>I</i>	2 × 10	1.6
NGC 3680 (South) .....		<i>V</i>	2 × 30	1.4
		<i>I</i>	2 × 10	1.3
NGC 3766 (Center) .....	1995 Jun 29	<i>V</i>	2 × 10	1.5
		<i>I</i>	1 × 1, 1 × 4, 1 × 5	1.5
NGC 6025 (Center) .....	1995 Jul 2	<i>V</i>	1 × 8, 1 × 10	1.5
		<i>I</i>	1 × 2, 1 × 3	1.6
NGC 6025 (South) .....		<i>V</i>	1 × 5, 1 × 8	1.6
		<i>I</i>	2 × 2	1.6
NGC 6067 (Center-West).....	1995 Jul 2	<i>V</i>	1 × 20, 1 × 60	1.4
		<i>I</i>	1 × 1, 1 × 5	1.4
NGC 6067 (Center-East) .....		<i>V</i>	1 × 20, 1 × 60	1.3
		<i>I</i>	1 × 1, 1 × 5, 1 × 30	1.3
NGC 6231 (South) .....	1995 Jun 30	<i>V</i>	2 × 2	1.6
		<i>I</i>	2 × 1	1.5
NGC 6231 (North) .....		<i>V</i>	1 × 1, 1 × 2	1.5
		<i>I</i>	2 × 0.3	1.5
NGC 6231 (Center) .....		<i>V</i>	1 × 1	1.7
		<i>I</i>	1 × 0.3	1.7
NGC 6242 (South) .....	1995 Jun 30	<i>V</i>	2 × 2	1.3
		<i>I</i>	1 × 0.3, 1 × 1	1.2
NGC 6242 (North) .....		<i>V</i>	2 × 2	1.3
		<i>I</i>	2 × 1	1.4
NGC 6259 (South) .....	1995 Jun 30	<i>V</i>	2 × 30	1.4
		<i>I</i>	2 × 10	1.4
NGC 6259 (North) .....		<i>V</i>	2 × 30	1.4
		<i>I</i>	2 × 10	1.4
IC 4651 (South).....	1995 Jun 30	<i>V</i>	2 × 30	1.4
		<i>I</i>	2 × 10	1.4
IC 4651 (North) .....		<i>V</i>	2 × 30	1.4
		<i>I</i>	2 × 10	1.4
NGC 6451 (Center) .....	1995 Jul 2	<i>V</i>	2 × 30, 1 × 120	1.6
		<i>I</i>	1 × 5, 1 × 30, 1 × 40	1.4
NGC 6633 (South) .....	1995 Jun 30	<i>V</i>	2 × 5	1.3
		<i>I</i>	2 × 1	1.2
NGC 6633 (West) .....		<i>V</i>	2 × 5	1.2
		<i>I</i>	2 × 1	1.2
NGC 6633 (East) .....		<i>V</i>	2 × 5	1.3
		<i>I</i>	2 × 1	1.2

deviation  $\sigma(V)$ , the color  $V-I$ , the standard deviation  $\sigma(V-I)$ , and the number of independent measures obtained for each star.

3. COMPOSITE  $M_v$  VERSUS  $(V-I)_0$  DIAGRAM

The procedure followed to obtain the empirical isochrones in the  $M_v$  versus  $(V-I)_0$  plane included the following steps: (1) Tracing of fiducial sequences in the observed  $V$  versus  $V-I$  diagrams of the template clusters. (2) Transformation of the observed  $V$  versus  $V-I$  diagrams into the  $M_v$  versus  $(V-I)_0$  plane. (3) Definition of mean sequences for clusters with nearly similar age. (4) Application of small corrections in absolute magnitude and/or intrinsic color to

ensure the internal coherence among all the isochrones. The observed  $V$  versus  $V-I$   $C-M$  diagrams for all clusters are presented in Figures 1a and 1b. To determine the fiducial positions of the template clusters' sequences, the observed  $C-M$  diagrams were used to obtain the  $V$  and  $V-I$  values corresponding to the most populated regions in the cluster sequences in which it is thought that "single stars" should be placed, allowing for some scatter due to observational errors. These points do not form a lower envelope but, rather, a mean sequence. The clusters' main sequences (MSs) are in general well defined, covering an appreciable range in  $V$  magnitude. They show different shapes due to the pronounced differences in the cluster ages. To improve

TABLE 3  
TRANSFORMATION COEFFICIENTS

Date (UT)	$v_1$	$v_2$	$v_3$	$i_1$	$i_2$	$i_3$
1995 Jun 29.....	5.957	-0.060	-0.017	5.462	-0.062	-0.063
	±0.221	±0.068	±0.025	±0.162	±0.028	±0.017
1995 Jun 30.....	5.931	-0.030	-0.019	5.492	-0.090	0.091
	±0.402	±0.054	±0.010	±0.330	±0.092	±0.010
1995 Jul 2.....	5.915	0.015	-0.044	5.463	-0.060	-0.075
	±0.064	±0.053	±0.004	±0.077	±0.065	±0.005

TABLE 4

MAGNITUDES AND COLORS OF STARS IN THE FIELD OF NGC 3680

Star	<i>X</i>	<i>Y</i>	<i>V</i>	$\sigma_V$	<i>V</i> − <i>I</i>	$\sigma(V-I)$	<i>n</i>
1	882.71	96.71	9.902	0.001	1.282	0.012	2
2	622.94	161.44	12.847	0.017	0.624	0.013	2
3	614.99	184.13	15.107	0.015	0.871	0.010	2
4	696.82	271.74	11.969	0.014	0.583	0.005	2
5	579.72	322.11	15.346	0.060	1.141	0.063	2
6	799.50	370.14	13.409	0.006	0.655	0.019	2
7	803.43	387.35	15.533	0.037	0.867	0.041	2
8	671.32	393.00	13.077	0.017	0.587	0.001	2
9	601.80	418.52	12.729	0.010	0.586	0.002	2
10	489.74	481.16	13.567	0.026	0.602	0.021	4
11	456.02	131.77	14.951	0.010	0.754	0.019	4
12	640.07	296.22	13.051	0.010	0.610	0.009	2
13	899.70	313.67	12.949	0.001	0.533	0.014	2
14	574.30	315.24	13.524	0.030	0.594	0.028	2
15	608.75	325.94	15.503	0.004	1.301	0.046	2
16	651.36	377.63	10.539	0.020	1.020	0.007	2
17	723.19	389.85	12.992	0.019	0.613	0.014	2
18	607.97	407.92	16.636	0.038	1.102	0.005	2
19	406.01	421.11	15.467	0.062	1.023	0.062	4
20	479.41	448.37	13.609	0.031	0.619	0.026	4
21	464.87	486.04	13.697	0.026	0.693	0.017	4
22	489.39	536.30	13.875	0.020	0.730	0.016	2
23	691.12	275.14	12.507	0.021	0.593	0.013	2
24	833.44	517.88	13.265	0.003	0.644	0.019	2
25	406.29	522.63	15.797	0.002	0.832	0.019	2
26	635.22	443.16	11.829	0.010	0.634	0.007	2
27	500.48	235.45	16.668	0.046	1.070	0.015	3
28	363.89	138.21	16.680		1.641		1
29	311.41	216.55	15.332	0.013	0.971	0.032	2
30	256.73	229.69	15.105	0.013	0.779	0.047	2
31	384.06	264.29	11.940	0.010	0.645	0.033	2
32	224.16	299.26	10.718		1.266	0.019	2
33	40.21	318.03	15.321	0.018	0.930	0.069	2
34	331.15	335.32	16.737		0.904		1
35	362.36	394.25	10.897	0.007	1.259	0.029	2
36	182.50	440.68	15.668	0.012	1.071	0.026	2
37	37.27	481.77	13.218	0.031	1.991	0.053	2
38	139.00	173.57	15.806	0.053	1.021	0.111	2
39	7.96	183.07	16.905		1.147		1
40	157.49	222.20	16.623	0.077	1.399	0.059	2
41	223.21	334.81	16.999	0.048	1.197	0.062	2
42	223.84	426.34	15.824	0.027	0.876	0.076	2
43	184.78	489.41	14.072	0.001	0.731	0.010	2
44	139.46	347.34	17.659		2.829		1
45	441.81	410.22	17.533		1.886		1
46	433.00	479.77	17.930		1.271		1

TABLE 5

MAGNITUDES AND COLORS OF STARS IN THE FIELD OF NGC 3766

Star	<i>X</i>	<i>Y</i>	<i>V</i>	$\sigma_V$	<i>V</i> − <i>I</i>	$\sigma(V-I)$	<i>n</i>
1	163.90	9.49	12.232	0.001	0.176	0.018	3
2	193.42	13.42	16.246		0.945		1
3	288.87	53.44	12.753	0.007	0.187	0.025	3
4	325.05	68.85	11.505	0.003	0.113	0.018	3
5	365.48	82.28	12.558	0.001	0.198	0.033	3
6	274.46	110.30	13.247	0.003	0.184	0.041	3
7	320.96	138.83	9.093	0.001	0.072	0.024	3
8	205.48	143.10	10.571	0.005	0.083	0.022	3
9	50.76	147.74	11.345	0.009	0.127	0.025	3
10	222.34	146.51	16.109	0.014	0.937	0.026	2
11	86.72	172.71	14.990	0.012	0.690	0.004	2
12	232.92	195.03	15.954		0.830		1
13	114.32	194.01	12.134	0.005	0.176	0.031	3
14	86.68	207.54	13.282	0.017	0.230	0.039	3
15	38.88	277.56	15.338	0.016	0.872	0.068	3
16	263.51	279.09	14.032	0.001	0.390	0.083	3
17	187.70	289.37	15.627	0.051	0.968	0.004	2
18	186.47	321.03	12.245	0.001	0.146	0.034	3
19	177.27	344.24	12.299	0.005	0.169	0.007	3
20	199.30	349.88	12.074	0.001	0.128	0.041	3
21	490.31	356.26	15.648	0.035	0.863	0.007	2
22	78.96	370.83	14.733	0.009	0.343	0.476	3
23	220.84	375.88	14.353	0.007	0.542	0.068	3
24	411.52	431.20	15.306	0.038	0.907	0.094	3
25	227.36	434.24	15.274	0.041	0.709	0.016	2
26	97.94	479.67	9.987	0.006	0.119	0.027	3
27	485.31	7.89	15.956	0.022	1.233	0.042	3
28	376.35	16.32	12.783	0.003	0.207	0.026	3
29	128.12	19.77	13.660	0.009	0.310	0.008	3
30	195.29	32.97	15.523	0.005	0.747	0.005	2
31	454.88	44.92	16.181	0.056	0.904	0.083	2
32	194.29	50.77	13.274	0.002	0.327	0.025	3
33	9.04	53.81	16.010	0.060	1.765	0.097	3
34	96.84	63.38	16.247		0.987		1
35	248.19	61.57	11.663	0.006	0.145	0.022	3
36	93.12	77.33	12.657	0.004	0.159	0.049	3
37	213.13	82.41	11.861	0.011	0.170	0.031	3
38	302.84	86.32	14.066	0.002	1.249	0.021	3
39	341.03	89.56	14.767	0.011	0.579	0.030	3
40	358.13	115.27	14.372	0.013	0.678	0.054	3
41	181.33	121.06	11.537	0.004	0.163	0.014	3
42	208.76	129.85	13.289	0.001	0.302	0.039	3
43	36.81	130.45	14.746	0.025	0.691	0.101	3
44	287.65	133.30	14.833	0.027	0.535	0.105	3
45	72.46	142.78	10.889	0.005	0.169	0.021	3
46	375.35	149.20	9.602	0.003	0.073	0.025	3
47	469.46	158.89	16.260		0.895		1
48	140.76	157.16	10.203	0.002	0.078	0.031	3
49	360.79	159.12	11.698	0.005	0.389	0.018	3
50	410.77	160.14	12.352	0.007	0.241	0.012	3
51	159.27	170.12	15.420	0.046	1.171	0.128	3
52	294.44	173.75	13.538	0.018	0.272	0.022	3
53	307.80	178.71	15.345	0.042	0.788	0.033	2
54	22.21	195.17	16.234	0.001	3.036	0.049	2
55	117.89	210.22	11.508	0.001	0.150	0.034	3
56	77.55	214.83	13.645	0.019	0.190	0.082	3
57	27.71	216.31	12.076	0.011	0.209	0.030	3
58	205.35	225.80	15.126	0.037	0.786	0.051	2
59	354.35	231.43	15.022	0.020	2.229	0.023	3
60	120.98	233.65	12.323	0.002	0.166	0.034	3
61	435.48	244.12	14.945	0.041	0.616	0.067	3
62	20.48	247.01	13.618	0.011	0.274	0.059	3
63	473.27	254.66	15.257	0.041	0.743	0.011	3
64	371.82	258.17	13.497	0.002	0.235	0.047	3
65	82.04	264.65	11.937	0.001	0.143	0.031	3
66	329.90	270.97	14.695	0.037	0.651	0.056	3
67	57.24	270.55	9.880	0.004	0.112	0.025	3
68	466.64	274.17	15.378	0.056	0.761	0.090	2
69	152.04	279.68	13.554	0.008	0.386	0.044	3
70	62.52	290.18	15.797		0.851		1
71	479.07	294.36	14.818	0.010	0.649	0.012	2
72	319.00	301.28	15.801		0.804		1
73	160.39	295.18	15.807	0.011	0.873	0.068	2

the determination of fiducial points in the *C*-*M* diagram of NGC 6633—the template with the smallest number of stars per square arcminute—the stars with the highest proper motion membership probabilities (Sanders 1973) were used. A similar treatment was performed for the MS stars of NGC 3680 for which proper motions (Kozhurina-Platais et al. 1995) and Coravel radial velocities (Nordström, Andersen, & Andersen 1996) are available. Finally, regarding the MS stars of NGC 6242, we have taken into account their membership status assigned by Moffat & Vogt (1973). The sets of fiducial points in each cluster are formed by (*V*, *V*−*I*) pairs chosen in such a way that two consecutive points differ in 0.5 mag in *V*. In some old template clusters, however, the fiducial points are defined for intervals of 0.25 mag, especially for the upper MSs with large variations in *V*−*I*. The fiducial sequences were then obtained by joining the fiducial points in each *C*-*M* diagram by allowing small curvatures between adjacent points. To define the fiducial points in the faintest regions of the *C*-*M* diagrams, the global behavior of the zero-age main sequence (ZAMS) for

TABLE 5—Continued

Star	X	Y	V	$\sigma V$	V-I	$\sigma(V-I)$	n
74	386.59	300.55	11.289	0.007	0.094	0.031	3
75	492.81	301.50	12.883	0.015	0.181	0.030	3
76	296.72	303.92	8.408	0.004	0.071	0.042	3
77	189.38	310.01	15.186	0.001	0.674	0.007	2
78	122.19	314.29	12.731	0.003	0.264	0.012	3
79	90.85	323.63	12.209	0.007	0.191	0.032	3
80	392.37	325.42	16.004	0.007	0.881	0.004	2
81	303.82	332.70	12.841	0.023	0.159	0.033	3
82	48.25	333.52	9.232	0.006	0.212	0.022	3
83	392.96	338.01	14.638	0.006	0.559	0.048	3
84	340.41	340.42	15.855	0.003	1.288	0.132	2
85	324.48	340.98	9.230	0.002	0.071	0.022	3
86	381.12	348.49	13.530	0.029	0.174	0.069	3
87	361.77	350.25	11.159	0.002	0.070	0.030	3
88	314.69	356.65	12.672	0.013	0.295	0.040	3
89	278.33	358.87	13.245	0.008	0.233	0.012	3
90	295.53	364.75	13.289	0.015	0.284	0.062	3
91	489.23	377.59	14.259	0.015	0.453	0.028	3
92	246.49	383.75	12.824	0.003	0.195	0.014	3
93	492.72	427.55	14.757	0.030	0.473	0.107	3
94	200.25	441.98	14.968	0.020	0.756	0.041	3
95	112.81	444.13	14.092	0.003	1.530	0.025	3
96	270.87	445.25	14.815	0.004	1.698	0.035	3
97	494.82	453.50	15.609	0.015	3.711	0.027	3
98	79.76	458.40	12.544	0.014	0.159	0.033	3
99	389.86	460.22	13.863	0.003	0.291	0.016	3
100	40.76	462.56	12.832	0.006	0.164	0.057	3
101	325.49	463.80	12.590	0.007	0.137	0.023	3
102	122.80	472.56	14.052	0.015	1.146	0.072	3
103	9.51	490.01	16.110	0.083	0.940	0.069	2
104	487.01	493.94	12.129	0.009	0.166	0.023	3
105	470.76	493.02	15.242	0.054	0.905	0.048	2
106	300.60	496.14	14.036	0.008	2.700	0.028	3
107	177.66	6.37	14.093	0.020	0.796	0.044	3
108	435.67	14.96	15.595	0.040	0.831	0.058	2
109	322.22	151.89	10.656	0.004	0.057	0.026	3
110	66.88	156.95	14.783	0.012	0.895	0.063	3
111	252.66	165.64	13.024	0.010	0.214	0.042	3
112	169.64	189.12	12.177	0.007	0.172	0.022	3
113	128.71	192.15	11.126	0.001	0.123	0.032	3
114	313.81	199.61	9.965	0.008	0.032	0.021	3
115	105.08	234.59	15.358	0.010	1.718	0.058	3
116	255.58	240.96	11.062	0.001	0.111	0.022	3
117	359.29	249.53	12.046	0.002	0.119	0.029	3
118	115.17	253.66	14.071	0.001	0.417	0.055	3
119	144.74	285.62	14.747	0.017	0.760	0.052	3
120	251.64	288.16	13.957	0.019	0.377	0.022	3
121	140.26	312.24	13.008	0.003	0.219	0.026	3
122	276.84	327.11	11.156	0.011	0.098	0.031	3
123	31.04	361.88	11.806	0.003	0.219	0.023	3
124	319.02	378.50	15.078	0.004	0.949	0.027	3
125	436.35	415.32	10.032	0.009	0.033	0.026	3
126	297.03	438.16	11.431	0.010	0.073	0.032	3
127	84.85	453.74	13.154	0.011	0.186	0.055	3
128	45.97	474.77	13.007	0.003	0.275	0.028	3
129	358.58	479.97	16.270		0.953		1
130	312.93	501.42	14.228	0.016	0.517	0.069	3
131	443.07	26.63	15.256	0.011	0.923	0.067	2
132	206.67	167.44	13.961	0.018	0.331	0.048	3
133	212.89	206.95	14.819	0.003	0.717	0.021	3
134	281.53	220.34	15.674	0.071	0.892	0.030	2
135	406.46	238.09	10.394	0.004	0.078	0.028	3
136	329.53	265.54	14.828	0.034	0.596	0.030	3
137	240.55	213.64	15.039	0.025	0.740	0.047	3
138	108.50	485.19	13.657	0.010	0.787	0.072	3
139	244.18	489.13	15.740	0.043	0.802	0.010	2
140	93.35	32.59	15.352	0.007	0.760	0.013	2
141	105.25	250.92	16.148	0.035	1.025	0.010	2
142	22.62	403.45	11.383	0.006	0.128	0.023	3
143	34.61	40.80	17.718		2.910		1
144	448.18	377.90	15.474	0.091	0.663	0.130	2
145	314.67	296.37	15.224	0.004	0.659	0.012	2
146	360.12	422.70	8.139	0.003	-0.007	0.030	3
147	187.76	144.12	16.510		1.473		1
148	67.71	3.34	15.918		2.069		1

TABLE 5—Continued

Star	X	Y	V	$\sigma V$	V-I	$\sigma(V-I)$	n
149	34.76	37.29	15.358		0.567		1
150	491.14	69.97	15.932		0.727		1
151	262.15	218.64	15.756		0.776		1
152	323.55	309.96	15.691		0.688		1
153	458.85	350.07	16.765		1.109		1
154	240.62	499.02	16.414		1.250		1
155	62.10	283.12	17.071		1.957		1
156	213.84	336.97	16.772		1.661		1
157	176.10	506.17	12.981		0.227		1
158	502.88	362.82	10.682		0.025		1

the brighter magnitudes was taken into account by avoiding breaks and/or abrupt changes in the shape of the sequences due to the presence of field stars. We have also traced the upper portions of the MSs on the basis of the positions of cluster members, i.e., we have not extrapolated toward the more evolved zones. Finally, we demarcated the giant clump region in the intermediate-age template clusters. Since the number of giants in each  $C-M$  diagram depends on the degree of completeness of the observed cluster field, this number does not always reflect the full behavior of the most evolved phases. However, the availability of  $VI$  data for some high-luminosity late-type stars in intermediate-age clusters at least allows us to draw the regions in the  $M_v$  versus  $(V-I)_0$  plane in which those stars are concentrated. The membership status of the observed giant stars in each cluster was taken from previous studies, mostly based on Coravel radial velocities, i.e., NGC 3680 and IC 4651 (Mermilliod et al. 1995), NGC 6067 (Mermilliod, Mayor, & Burki 1987), and NGC 6259 (Piatti et al. 1995; J. C. Mermilliod 1997, private communication). The transformation of the observed  $V$  versus  $V-I$  diagram into the  $M_v$  versus  $(V-I)_0$  plane for each template requires the knowledge of its reddening and distance. In general, if a cluster has unreliable determinations of reddening and distance but precise photometric measurements, its MS will appear shifted in  $M_v$  and/or  $(V-I)_0$  with respect to the MSs of template clusters with accurate reddening and distance determinations. If there exist differences not only in the  $M_v$  and  $(V-I)_0$  zero points but also in the slope of the cluster MS from those of the other templates, then the photometric measurements may be affected by observational errors. The reddenings, distances, and ages of the template clusters were taken from different sources. The adopted fundamental parameters are shown in Table 14 together with the corresponding sources of reference. Whenever a quantity was taken from more than one reference, the average of all the determinations was adopted, and we have assigned higher weights to the highest quality values. As shown in Table 14, all the template clusters are of nearly solar metal content. The  $E(V-I)$  color excess of each template was calculated from the adopted  $E(B-V)$  color excess listed in Table 14, using the ratio  $E(V-I)/E(B-V) = 1.25$  given by Walker (1985a). Then, the intrinsic  $(V-I)_0$  colors for all the fiducial points in each template were obtained. The corresponding  $M_v$  absolute magnitudes were derived from the adopted distance moduli of the clusters. The unevolved MSs of the 10 template clusters were used to define the empirical ZAMS in the  $M_v$  versus  $(V-I)_0$  plane, which cover the absolute magnitude range from  $M_v \sim -3.5$  to approximately 9 (Fig. 2). The upper part of the ZAMS is mainly defined by the fiducial sequence of the very young cluster

TABLE 6

MAGNITUDES AND COLORS OF STARS IN THE FIELD OF NGC 6025

Star	X	Y	V	$\sigma V$	V-I	$\sigma(V-I)$	n
1	1124.23	261.42	15.445	0.025	1.005	0.005	2
2	1095.16	272.06	12.930	0.010	0.485	0.005	2
3	891.63	363.62	14.950	0.100	1.065	0.115	2
4	1098.97	463.57	15.870		1.180		1
5	1322.56	640.63	12.525	0.005	0.585	0.015	2
6	980.31	692.48	16.380		1.350		1
7	928.49	256.69	14.655	0.035	0.865	0.045	2
8	962.87	311.99	13.985	0.005	1.520	0.030	2
9	905.67	350.62	16.120		0.730		1
10	1047.38	357.59	15.470	0.070	1.560	0.080	2
11	1253.63	367.37	9.195	0.005	0.040	0.020	2
12	1097.64	410.89	13.645	0.015	0.955	0.015	2
13	1332.80	426.02	15.760	0.200	0.995	0.285	2
14	1213.39	435.49	13.165	0.005	0.675	0.005	2
15	1162.55	438.84	11.230	0.001	0.295	0.025	2
16	1084.68	510.96	13.755	0.015	2.050	0.040	2
17	1017.60	528.91	8.120	0.010	0.075	0.035	2
18	1072.65	537.49	16.040		0.790		1
19	885.32	542.65	14.725	0.015	1.415	0.035	2
20	1128.63	545.87	15.960		1.550		1
21	996.71	571.12	13.790	0.020	0.705	0.035	2
22	1305.34	585.01	14.075	0.045	0.800	0.040	2
23	885.64	595.33	16.100		1.150		1
24	1207.18	648.74	15.800		1.390		1
25	1019.90	700.00	9.875	0.005	0.095	0.025	2
26	943.22	722.39	14.735	0.035	1.515	0.045	2
27	869.96	328.03	14.980	0.050	0.840	0.080	2
28	1330.34	417.24	16.000		1.420		1
29	1299.51	447.00	14.310	0.010	0.795	0.015	2
30	948.54	479.91	15.670	0.040	1.050	0.020	2
31	1024.38	501.08	12.840		0.490		1
32	1137.30	516.04	15.950		1.010		1
33	1334.32	543.04	16.250		1.560		1
34	1231.43	553.74	8.890	0.001	0.080	0.020	2
35	1281.03	594.65	13.900	0.010	1.460	0.030	2
36	1038.58	633.01	12.735	0.005	0.460	0.001	2
37	953.73	490.65	16.270		0.900		1
38	891.86	657.23	15.490		1.130		1
39	359.71	107.08	14.915	0.055	0.900	0.070	2
40	267.50	224.62	15.180		0.940		1
41	118.11	36.77	15.840		1.650		1
42	434.23	77.70	14.630	0.010	2.625	0.005	2
43	232.80	103.83	13.165	0.005	0.670	0.001	2
44	108.91	212.32	11.775	0.015	0.230	0.010	2
45	42.55	394.05	15.860		1.220		1
46	155.24	457.88	15.190	0.020	1.005	0.085	2
47	391.43	481.88	15.115	0.005	1.610	0.020	2
48	324.94	34.39	13.870	0.020	1.175	0.025	2
49	84.75	49.80	14.700		1.560		1
50	7.86	299.52	15.560		0.950		1
51	181.75	307.02	13.490		0.690		1
52	20.44	310.69	11.300		0.320		1
53	478.92	312.75	14.310		0.860		1
54	94.68	363.72	13.585	0.015	2.095	0.005	2
55	362.86	373.94	8.410	0.020	0.065	0.035	2
56	65.01	409.90	12.820		0.680		1
57	2.61	489.17	14.850		2.250		1
58	223.74	490.55	9.755	0.025	0.060	0.030	2
59	145.87	113.56	8.155	0.015	0.045	0.025	2
60	265.98	113.47	7.315	0.005	-0.030	0.010	2
61	182.78	306.34	13.460		0.670		1
62	21.48	309.90	11.270		0.240		1
63	479.94	312.09	14.360		0.920		1
64	3.72	488.73	14.860		2.230		1
65	85.79	49.23	14.680		1.530		1
66	268.62	223.66	15.320		1.110		1
67	66.02	409.13	12.800		0.590		1

TABLE 7

MAGNITUDES AND COLORS OF STARS IN THE FIELD OF NGC 6067

Star	X	Y	V	$\sigma V$	V-I	$\sigma(V-I)$	n
1	247.55	468.97	12.740	0.006	0.803	0.028	5
2	129.85	500.47	12.470	0.026	0.407	0.027	5
3	502.47	516.74	11.996	0.002	0.431	0.025	2
4	220.97	526.44	16.807	0.067	3.842	0.038	2
5	95.57	537.46	14.498	0.016	0.615	0.019	2
6	189.30	546.31	11.402	0.002	0.373	0.019	2
7	183.68	568.68	13.156	0.007	0.440	0.038	2
8	73.92	602.30	12.840	0.002	0.411	0.010	2
9	347.00	610.87	13.888	0.010	0.447	0.035	2
10	140.93	695.41	14.696	0.039	1.583	0.001	2
11	87.06	707.31	14.517	0.020	1.406	0.028	2
12	515.68	752.75	11.581	0.001	1.433	0.051	2
13	565.53	769.66	14.068	0.001	0.358	0.108	2
14	514.05	782.43	14.185	0.010	0.525	0.091	2
15	230.65	783.28	11.884	0.002	0.358	0.049	2
16	192.96	799.71	14.749	0.011	1.725	0.035	2
17	426.53	805.21	16.498	0.012	2.859	0.023	2
18	207.78	856.57	14.755	0.005	1.680	0.076	2
19	397.52	856.56	14.503	0.005	0.515	0.063	2
20	123.09	873.11	13.565	0.007	0.438	0.051	2
21	497.73	895.03	13.053	0.011	0.488	0.001	2
22	163.99	903.82	15.255	0.018	1.651	0.074	2
23	335.55	910.38	12.592	0.001	0.447	0.028	2
24	301.10	932.57	13.922	0.002	0.413	0.073	2
25	543.99	947.18	13.331	0.006	0.410	0.058	2
26	150.68	462.75	12.929	0.009	0.377	0.024	5
27	518.30	464.19	14.383	0.016	0.463	0.125	2
28	385.45	468.53	12.616	0.008	0.326	0.018	5
29	217.24	471.62	8.524	0.011	1.345	0.052	4
30	441.83	500.89	13.576	0.015	1.714	0.033	5
31	405.09	502.25	14.392	0.029	1.393	0.050	5
32	76.74	504.98	14.826	0.010	1.558	0.069	4
33	493.08	519.94	13.082	0.005	0.458	0.014	2
34	518.82	523.27	15.231	0.024	1.524	0.031	2
35	527.34	535.58	11.230	0.003	0.388	0.018	2
36	433.61	535.63	14.967	0.017	1.598	0.032	2
37	348.61	536.52	11.981	0.003	0.391	0.030	2
38	148.75	542.97	15.294	0.043	1.580	0.009	2
39	368.53	543.63	13.861	0.018	0.500	0.060	2
40	472.80	548.95	14.345	0.010	0.633	0.046	2
41	290.37	551.66	14.229	0.002	0.470	0.025	2
42	277.20	569.30	12.345	0.002	0.434	0.015	2
43	469.34	580.01	10.920	0.003	0.426	0.038	2
44	522.46	583.36	12.611	0.003	0.409	0.006	2
45	492.10	594.29	14.924	0.008	1.225	0.023	2
46	420.28	604.73	12.969	0.002	0.482	0.022	2
47	530.41	610.53	14.471	0.030	0.621	0.027	2
48	293.04	612.82	13.724	0.003	0.405	0.058	2
49	181.10	617.89	14.245	0.001	0.711	0.068	2
50	152.45	619.80	14.024	0.006	0.288	0.131	2
51	420.64	627.15	13.897	0.001	0.447	0.086	2
52	189.54	628.80	12.515	0.004	1.600	0.010	2
53	250.85	654.09	12.252	0.004	0.390	0.009	2
54	99.43	662.32	10.908	0.003	0.307	0.024	2
55	140.27	667.13	12.997	0.010	0.379	0.031	2
56	314.22	671.38	13.267	0.003	0.372	0.042	2
57	425.73	674.90	14.569	0.005	1.720	0.016	2
58	407.79	678.76	12.627	0.002	0.415	0.016	2
59	412.65	680.48	13.830	0.007	0.614	0.008	2
60	235.40	679.72	14.438	0.009	1.448	0.002	2
61	85.70	687.09	13.779	0.017	0.319	0.064	2
62	219.04	687.46	11.068	0.002	0.337	0.029	2
63	185.78	691.84	13.432	0.003	0.348	0.079	2
64	123.97	693.78	13.865	0.019	0.389	0.084	2
65	259.48	697.13	13.554	0.001	0.352	0.041	2
66	270.77	709.41	14.918	0.007	1.061	0.106	2
67	161.45	722.25	10.040	0.006	1.597	0.050	2
68	462.01	735.73	9.143		1.945		1
69	107.23	741.04	14.459	0.002	0.765	0.155	2
70	140.51	746.71	13.882	0.001	0.400	0.091	2
71	237.06	752.99	11.282	0.001	0.343	0.032	2
72	468.21	756.15	13.161	0.001	0.640	0.039	2
73	495.53	757.08	10.924	0.003	0.432	0.056	2

TABLE 7—Continued

Star	X	Y	V	$\sigma V$	V-I	$\sigma(V-I)$	n
74	341.52	767.17	10.602	0.005	0.390	0.051	2
75	74.80	773.25	13.568	0.014	0.465	0.018	2
76	516.62	773.41	13.331	0.002	0.448	0.024	2
77	281.48	778.02	11.648	0.004	0.411	0.039	2
78	348.58	783.48	14.220	0.001	0.676	0.029	2
79	566.59	791.25	14.913	0.006	0.604	0.198	2
80	535.65	806.12	14.833	0.001	1.553	0.016	2
81	556.91	810.41	9.014	0.019	0.326	0.039	2
82	288.84	815.19	13.455	0.011	0.441	0.009	2
83	197.29	826.47	12.965	0.003	0.419	0.023	2
84	241.40	832.89	14.536	0.019	0.629	0.054	2
85	568.50	834.34	14.095	0.013	0.426	0.031	2
86	170.90	861.65	11.699	0.004	0.425	0.020	2
87	483.69	874.48	13.619	0.003	1.469	0.005	2
88	395.71	882.21	12.375	0.002	0.467	0.017	2
89	318.28	892.61	11.693	0.001	0.517	0.033	2
90	483.63	898.68	13.157	0.004	1.594	0.025	2
91	385.10	900.42	13.310	0.005	1.514	0.038	2
92	102.59	906.76	14.722	0.030	0.555	0.077	2
93	353.95	907.28	14.719	0.008	0.785	0.121	2
94	475.41	907.95	15.277	0.031	1.900	0.031	2
95	345.40	940.41	13.728	0.005	0.503	0.001	2
96	171.10	543.26	11.962	0.008	0.405	0.041	2
97	222.61	640.95	12.284	0.005	1.901	0.034	2
98	509.11	644.82	11.991	0.002	0.453	0.024	2
99	254.62	665.88	13.527	0.018	0.376	0.052	2
100	170.41	725.67	9.698	0.003	2.026	0.050	2
101	206.84	918.65	15.330	0.016	1.626	0.124	2
102	263.81	550.41	12.399	0.001	0.831	0.012	2
103	338.74	878.47	8.751		1.807		1
104	111.42	468.30	14.507	0.005	0.615	0.021	3
105	563.04	480.61	15.248		0.578		1
106	318.89	484.04	15.773	0.031	0.898	0.059	3
107	286.14	495.15	14.307	0.013	0.582	0.028	3
108	368.21	500.63	14.374	0.012	0.591	0.017	3
109	464.35	505.03	16.852		1.347		1
110	524.03	506.06	15.243		0.805		1
111	237.48	506.57	16.576	0.266	1.083	0.214	3
112	170.10	507.39	16.170		1.058		1
113	475.17	531.42	15.005		0.680		1
114	409.60	542.16	15.112		0.894		1
115	544.86	544.17	16.355		0.822		1
116	377.35	546.73	16.921		1.650		1
117	389.83	573.48	15.783		0.948		1
118	519.76	594.63	16.352		0.912		1
119	351.71	596.77	16.497		0.659		1
120	110.15	610.50	17.095		1.653		1
121	447.23	611.89	16.696		1.020		1
122	238.18	619.29	15.162		0.889		1
123	132.63	645.42	14.555		0.819		1
124	289.55	659.19	16.675		1.408		1
125	558.27	693.27	16.466		1.176		1
126	468.01	698.59	16.645		1.131		1
127	423.75	704.84	15.968		1.804		1
128	381.97	729.31	16.235		1.139		1
129	118.74	750.62	14.607		0.625		1
130	379.23	768.58	16.096		1.753		1
131	216.87	839.53	15.414		0.788		1
132	236.83	861.49	14.634		0.698		1
133	233.94	871.30	15.247		0.802		1
134	367.73	924.69	15.849		0.835		1
135	136.61	941.98	15.122		0.794		1
136	485.97	461.79	15.922	0.089	0.940	0.167	3
137	82.81	465.29	15.206	0.035	0.744	0.041	3
138	470.00	474.42	15.215	0.017	0.797	0.030	3
139	276.73	479.98	16.598	0.065	1.048	0.081	3
140	435.71	480.51	16.884		1.187		1
141	532.38	489.66	15.536		0.820		1
142	199.82	489.78	14.972	0.042	0.759	0.049	3
143	565.40	490.96	16.741		2.110		1
144	466.77	492.14	14.922	0.025	0.960	0.035	3
145	424.35	502.79	16.975		2.222		1
146	148.81	510.93	14.465		0.680		1
147	168.39	518.21	17.070		3.115		1

TABLE 7—Continued

Star	X	Y	V	$\sigma V$	V-I	$\sigma(V-I)$	n
148	450.94	524.53	16.678		2.051		1
149	326.05	532.70	15.225		0.933		1
150	487.96	546.77	14.983		0.771		1
151	345.67	548.74	17.698		2.057		1
152	484.49	561.49	15.514		1.745		1
153	306.49	562.24	14.761		0.714		1
154	530.82	565.48	14.580		0.820		1
155	84.21	567.30	15.734		1.108		1
156	253.18	577.53	15.431		1.019		1
157	244.47	578.03	15.458		0.844		1
158	440.22	580.03	16.495		1.230		1
159	255.69	586.53	15.647		1.095		1
160	89.99	590.73	15.247		0.736		1
161	277.42	600.21	16.944		1.290		1
162	551.00	602.97	17.095		4.348		1
163	93.39	618.73	13.965		0.451		1
164	292.20	623.71	15.914		0.967		1
165	370.47	624.10	16.338		1.068		1
166	400.38	630.59	14.625		0.654		1
167	288.36	632.66	15.064		1.099		1
168	493.80	639.73	14.592		0.633		1
169	341.24	644.28	17.415		2.355		1
170	113.37	646.29	16.061		0.934		1
171	385.13	648.18	17.956		2.593		1
172	478.31	650.85	17.393		1.220		1
173	459.40	658.44	16.713		1.849		1
174	506.57	664.01	15.940		1.889		1
175	538.35	668.28	17.156		1.335		1
176	508.93	679.75	15.535		0.969		1
177	460.76	690.57	16.379		1.035		1
178	491.86	694.22	17.431		1.344		1
179	550.39	700.21	16.795		1.050		1
180	235.76	700.46	16.215		0.976		1
181	438.78	709.93	16.181		0.895		1
182	321.78	715.04	16.299		1.048		1
183	516.46	725.48	16.985		1.079		1
184	317.64	726.12	15.922		1.003		1
185	269.97	726.82	16.369		0.994		1
186	432.28	732.71	16.277		0.940		1
187	419.47	737.81	15.448		0.869		1
188	430.82	759.88	17.075		0.919		1
189	360.81	766.91	16.086		0.986		1
190	201.88	767.41	14.633		0.615		1
191	196.76	772.13	15.664		1.068		1
192	240.85	774.32	15.446		0.783		1
193	301.58	771.32	15.061		0.808		1
194	462.75	771.41	14.795		0.572		1
195	92.17	779.85	18.176		1.866		1
196	363.07	785.50	15.794		0.993		1
197	124.99	791.17	15.902		0.747		1
198	393.22	794.91	14.918		0.690		1
199	347.97	797.54	17.521		2.388		1
200	525.20	805.34	14.783		0.649		1
201	269.67	810.99	15.241		0.901		1
202	214.58	825.97	16.201		2.048		1
203	369.68	831.78	15.411		0.836		1
204	461.01	832.32	15.077		0.763		1
205	336.23	841.86	13.944		0.572		1
206	129.03	848.08	15.584		0.898		1
207	137.90	857.75	14.858		0.661		1
208	178.21	871.44	15.540		0.752		1
209	435.81	877.27	14.415		0.587		1
210	173.61	891.74	15.855		0.995		1
211	85.98	896.06	16.540		1.282		1
212	442.86	900.52	16.166		0.877		1
213	461.59	900.75	15.783		0.955		1
214	175.54	908.20	14.498		0.672		1
215	87.95	910.85	15.566		0.962		1
216	461.34	912.40	15.464		1.540		1
217	445.68	921.59	16.687		0.924		1
218	258.94	925.07	16.166		0.734		1
219	245.35	926.04	16.199		1.174		1
220	144.23	926.80	14.804		0.737		1
221	358.65	933.07	17.073		1.283		1

TABLE 7—Continued

Star	X	Y	V	$\sigma V$	V-I	$\sigma(V-I)$	n
222.....	273.14	935.92	15.644		0.787		1
223.....	162.23	938.10	15.800		1.607		1
224.....	523.63	943.84	15.568		0.818		1
225.....	386.50	944.08	16.042		0.923		1
226.....	128.05	945.09	14.187		0.558		1
227.....	509.40	954.89	16.217		0.963		1
228.....	496.42	956.82	15.189		0.807		1
229.....	470.41	958.62	17.414		1.602		1
230.....	131.28	960.42	17.118		1.755		1
231.....	545.08	532.70	16.832		0.877		1
232.....	71.12	541.62	16.659		1.948		1
233.....	248.73	543.28	16.748		1.075		1
234.....	517.52	545.45	15.824		0.945		1
235.....	502.37	605.93	15.198		1.117		1
236.....	454.82	610.65	17.068		1.222		1
237.....	226.32	645.23	13.621		0.425		1
238.....	270.61	690.75	15.274		0.876		1
239.....	224.73	695.18	14.933		0.465		1
240.....	147.48	700.67	15.893		0.887		1
241.....	502.93	719.88	17.022		1.391		1
242.....	559.46	725.50	17.014		1.421		1
243.....	415.22	762.48	16.578		1.036		1
244.....	391.90	837.43	15.326		0.935		1
245.....	488.18	848.98	15.529		0.866		1
246.....	271.65	855.89	16.603		1.028		1
247.....	76.18	865.80	16.805		0.990		1
248.....	188.85	879.84	16.071		1.132		1
249.....	162.17	917.24	17.574		1.188		1
250.....	72.66	957.69	14.743		1.001		1
251.....	463.03	591.07	16.592		1.861		1
252.....	96.03	826.03	17.285		1.314		1
253.....	328.60	634.73	17.520		3.189		1
254.....	457.32	490.04	15.697	0.061	1.745	0.150	3
255.....	394.44	733.00	15.463		0.867		1
256.....	331.65	851.95	16.726		1.896		1
257.....	494.37	457.84	13.616	0.011	0.493	0.036	4
258.....	462.38	25.92	15.927	0.043	1.008	0.049	2
259.....	62.90	41.64	14.639	0.014	0.626	0.015	2
260.....	46.22	56.73	16.415	0.121	1.211	0.151	2
261.....	379.25	60.83	16.240	0.132	1.327	0.041	2
262.....	386.46	65.58	16.161	0.091	1.357	0.139	2
263.....	375.61	86.61	16.606	0.141	2.131	0.163	2
264.....	443.95	102.67	14.491	0.023	0.635	0.060	3
265.....	124.97	184.93	12.315	0.004	0.542	0.030	3
266.....	125.20	192.29	12.728	0.006	0.509	0.030	3
267.....	433.68	197.45	15.790	0.063	1.238	0.082	2
268.....	74.18	216.72	15.333	0.077	1.188	0.113	2
269.....	119.00	217.19	14.583	0.001	0.634	0.012	2
270.....	326.59	223.83	16.005	0.032	1.219	0.050	2
271.....	411.91	245.34	14.823	0.018	0.679	0.020	2
272.....	168.13	255.87	16.075	0.043	1.136	0.072	2
273.....	35.78	306.33	15.468	0.015	0.968	0.009	2
274.....	360.87	312.91	15.629	0.056	2.003	0.101	3
275.....	452.74	318.93	16.632	0.081	1.218	0.122	2
276.....	134.89	334.60	14.563	0.007	0.608	0.015	2
277.....	392.03	336.97	14.998	0.017	0.885	0.136	3
278.....	121.26	361.41	15.928	0.062	1.107	0.105	2
279.....	415.04	367.28	14.352	0.008	0.744	0.064	3
280.....	437.69	373.16	12.773	0.004	0.330	0.023	3
281.....	487.55	392.55	12.658	0.008	0.294	0.037	3
282.....	387.42	402.50	13.559	0.006	1.652	0.027	3
283.....	257.61	410.22	15.938	0.021	2.471	0.055	3
284.....	421.29	419.68	11.729	0.003	0.357	0.032	3
285.....	479.24	420.41	14.973	0.007	0.662	0.024	2
286.....	409.84	422.16	14.052	0.026	0.685	0.063	3
287.....	386.15	431.43	11.598	0.006	0.322	0.030	3
288.....	304.99	441.88	14.743	0.032	0.683	0.054	2
289.....	388.96	451.86	11.648	0.002	0.400	0.050	3
290.....	406.84	453.75	10.963	0.005	0.388	0.044	3
291.....	306.82	13.21	15.715	0.049	0.972	0.045	2
292.....	307.84	20.18	15.202	0.031	0.938	0.036	3
293.....	344.45	16.21	14.773	0.040	0.708	0.035	2
294.....	128.87	16.97	16.268	0.146	1.229	0.198	2
295.....	126.45	23.02	16.343	0.056	1.011	0.036	2
296.....	465.70	32.28	13.953	0.015	0.767	0.037	3

TABLE 7—Continued

Star	X	Y	V	$\sigma V$	V-I	$\sigma(V-I)$	n
297.....	147.16	36.74	14.892	0.010	1.694	0.065	3
298.....	466.96	44.51	16.159	0.046	1.667	0.062	2
299.....	125.49	51.02	16.056	0.047	1.304	0.084	2
300.....	4.15	62.87	16.225	0.145	1.324	0.183	2
301.....	175.23	75.67	14.144	0.009	0.494	0.077	3
302.....	11.09	87.05	15.987	0.040	1.255	0.039	2
303.....	146.66	88.12	14.637	0.003	0.716	0.035	2
304.....	483.97	89.04	15.220	0.081	0.944	0.203	2
305.....	378.24	114.45	15.560	0.070	0.943	0.087	2
306.....	125.28	122.96	15.860	0.069	1.108	0.107	2
307.....	118.08	142.54	16.755	0.198	1.313	0.240	2
308.....	55.67	146.27	15.148	0.045	0.862	0.065	2
309.....	200.93	148.17	16.165	0.049	1.115	0.116	2
310.....	12.25	152.38	14.433	0.012	0.536	0.178	3
311.....	346.62	152.41	14.788	0.008	1.071	0.025	3
312.....	244.67	161.71	15.302	0.023	1.250	0.035	2
313.....	374.68	170.30	12.802	0.005	0.497	0.022	3
314.....	442.91	175.71	11.783	0.002	0.392	0.038	3
315.....	487.31	177.67	14.233	0.011	0.481	0.068	3
316.....	213.36	180.95	12.820	0.005	0.516	0.021	3
317.....	217.95	187.94	13.767	0.006	0.539	0.058	3
318.....	166.41	187.95	14.883	0.046	0.744	0.064	2
319.....	467.61	190.87	14.854	0.023	1.274	0.088	3
320.....	257.78	192.62	15.662	0.073	0.948	0.082	2
321.....	156.32	198.75	12.173	0.004	0.505	0.031	3
322.....	441.08	201.26	16.017	0.054	1.048	0.035	2
323.....	4.19	204.25	15.691	0.070	0.993	0.100	2
324.....	315.97	218.17	14.236	0.018	1.031	0.032	2
325.....	172.11	218.69	15.829	0.087	1.081	0.137	2
326.....	450.07	235.99	15.595	0.065	1.055	0.093	2
327.....	96.42	238.30	15.031	0.018	0.853	0.042	2
328.....	427.65	238.68	13.511	0.008	0.392	0.061	3
329.....	240.02	242.89	15.844	0.054	1.078	0.072	2
330.....	403.62	250.65	12.249	0.003	0.404	0.033	3
331.....	53.30	262.52	14.014	0.023	0.662	0.106	3
332.....	441.21	277.90	16.569	0.031	3.580	0.049	3
333.....	212.89	278.71	15.406	0.052	0.992	0.060	2
334.....	181.98	282.06	14.402	0.018	0.861	0.134	3
335.....	505.50	285.84	15.921		1.279		1
336.....	324.96	287.70	16.949	0.133	1.608	0.425	2
337.....	225.39	288.41	10.758	0.002	0.467	0.038	3
338.....	198.80	292.34	15.035	0.018	1.586	0.084	3
339.....	157.60	301.84	12.490	0.009	0.474	0.042	3
340.....	500.27	305.15	12.042	0.006	0.291	0.023	3
341.....	336.39	306.58	15.259	0.060	1.174	0.083	2
342.....	293.75	307.38	15.830	0.058	1.184	0.036	2
343.....	182.16	314.06	15.468	0.012	0.828	0.001	2
344.....	341.37	321.90	14.859	0.001	0.651	0.005	2
345.....	410.93	330.42	13.653	0.010	0.402	0.065	3
346.....	400.63	330.80	15.623	0.038	0.951	0.081	2
347.....	360.45	334.44	14.143	0.014	0.749	0.128	3
348.....	165.30	336.29	14.920	0.016	1.023	0.054	2
349.....	434.26	336.71	16.795	0.072	1.168	0.016	2
350.....	220.41	346.77	13.376	0.007	0.416	0.020	3
351.....	268.08	347.86	10.070	0.002	1.793	0.045	2
352.....	423.63	353.95	14.520	0.007	1.539	0.041	3
353.....	133.68	356.60	13.615	0.018	0.409	0.026	3
354.....	456.46	356.72	15.870	0.035	0.854	0.031	2
355.....	183.94	356.90	15.251	0.018	0.807	0.056	2
356.....	288.98	356.84	16.398	0.087	1.186	0.108	2
357.....	335.60	364.63	15.694	0.073	0.887	0.068	2
358.....	475.64	371.53	15.143	0.018	1.090	0.041	2
359.....	370.74	375.46	12.165	0.004	0.399	0.049	3
360.....	327.18	375.79	13.393	0.009	0.515	0.014	3
361.....	256.45	379.02	15.035	0.013	0.683	0.013	2
362.....	32.43	381.81	12.456	0.008	0.350	0.045	3
363.....	206.68	382.19	14.984	0.001	0.898	0.025	2
364.....	396.11	383.50	15.984	0.101	0.972	0.123	2
365.....	231.62	384.27	13.110	0.005	0.408	0.022	3
366.....	380.50	386.39	13.752	0.008	0.482	0.036	3
367.....	26.64	389.64	12.376	0.004	0.397	0.026	3
368.....	288.98	396.03	12.727	0.004	0.384	0.023	3
369.....	441.56	400.50	15.141	0.026	0.766	0.048	2
370.....	124.79	405.07	15.793	0.053	0.942	0.063	2
371.....	411.05	410.87	15.015	0.018	1.551	0.048	3



TABLE 7—Continued

Star	X	Y	V	$\sigma V$	V-I	$\sigma(V-I)$	n
372.....	189.87	424.05	16.201	0.099	0.932	0.116	2
373.....	301.91	426.79	15.548	0.012	0.850	0.022	2
374.....	112.74	442.38	16.492	0.088	1.468	0.113	2
375.....	201.95	443.69	11.163	0.002	0.380	0.054	3
376.....	336.97	448.32	14.139	0.010	0.516	0.044	2
377.....	220.51	450.27	8.980	0.002	0.746	0.041	2
378.....	68.99	461.73	13.401	0.010	0.398	0.048	3
379.....	67.96	487.15	11.146	0.003	0.349	0.043	3
380.....	454.61	500.95	16.276	0.072	0.991	0.010	2
381.....	64.53	139.09	13.866	0.024	0.554	0.051	3
382.....	379.91	176.70	16.187		0.982		1
383.....	372.49	191.04	11.373	0.008	0.466	0.039	3
384.....	193.89	205.29	15.155	0.033	1.029	0.025	2
385.....	220.89	275.75	15.635	0.053	0.952	0.054	2
386.....	254.74	282.30	15.847	0.038	1.298	0.049	2
387.....	214.86	318.82	15.722	0.036	0.916	0.030	2
388.....	288.65	334.98	16.107	0.063	1.192	0.114	2
389.....	92.27	336.37	15.853	0.026	1.860	0.059	2
390.....	241.14	342.05	10.579	0.002	0.321	0.054	3
391.....	206.51	415.17	15.137	0.042	0.765	0.076	2
392.....	13.72	444.75	15.708	0.019	0.859	0.001	2
393.....	459.49	485.15	15.641		0.893		1
394.....	312.95	35.16	15.883		0.946		1
395.....	80.18	35.67	16.615		1.878		1
396.....	363.17	42.55	17.416		1.136		1
397.....	484.75	51.73	17.865		2.484		1
398.....	428.20	57.21	17.533		1.254		1
399.....	433.69	77.24	17.721		1.151		1
400.....	260.27	110.97	16.540		3.436		1
401.....	499.69	131.92	16.973		1.033		1
402.....	290.27	140.85	16.479		1.167		1
403.....	402.42	166.26	16.720		1.325		1
404.....	104.81	172.03	16.781		2.987		1
405.....	426.09	186.11	17.882		1.182		1
406.....	174.82	189.86	15.693		0.912		1
407.....	233.87	251.52	16.795		1.122		1
408.....	296.57	266.89	17.659		1.316		1
409.....	238.80	303.89	17.839		2.638		1
410.....	42.08	319.10	17.064		1.235		1
411.....	8.64	347.87	18.034		1.407		1
412.....	167.70	368.49	17.237		1.263		1
413.....	453.65	390.60	17.618		1.048		1
414.....	433.51	407.19	16.741		0.857		1
415.....	178.18	419.47	16.536		1.060		1
416.....	359.77	439.18	15.961		3.837		1
417.....	59.48	449.76	15.824		0.975		1
418.....	435.87	481.06	16.760		1.048		1
419.....	236.72	23.79	16.825		1.109		1
420.....	171.05	26.93	16.905		1.242		1
421.....	295.67	42.79	17.569		0.942		1
422.....	265.60	42.99	17.674		1.342		1
423.....	193.33	57.67	17.649		2.841		1
424.....	143.39	64.63	16.595		1.270		1
425.....	259.50	70.57	16.053		3.097		1
426.....	261.47	75.88	16.429		2.201		1
427.....	150.76	72.26	16.298		1.224		1
428.....	503.15	72.98	18.125		1.106		1
429.....	98.88	73.50	17.202		1.082		1
430.....	423.07	78.65	16.933		1.177		1
431.....	322.78	80.50	17.834		1.365		1
432.....	192.08	85.85	17.558		1.148		1
433.....	173.81	95.65	17.151		1.148		1
434.....	385.48	100.39	17.495		1.477		1
435.....	282.60	110.92	17.783		1.238		1
436.....	417.65	118.47	17.438		2.546		1
437.....	156.24	118.78	17.255		1.292		1
438.....	331.70	129.22	16.975		1.052		1
439.....	9.18	129.81	16.520		1.179		1
440.....	274.28	142.06	17.560		1.293		1
441.....	420.74	147.08	16.570		1.115		1
442.....	400.25	149.50	17.049		1.346		1
443.....	26.32	150.24	16.984		1.132		1
444.....	335.84	150.78	15.858		1.100		1
445.....	99.26	162.13	16.658		0.983		1
446.....	145.72	179.81	17.325		1.280		1

TABLE 7—Continued

Star	X	Y	V	$\sigma V$	V-I	$\sigma(V-I)$	n
447.....	400.46	188.56	16.798		1.246		1
448.....	385.32	215.08	15.926		1.120		1
449.....	42.86	216.85	17.038		1.299		1
450.....	227.95	219.61	16.864		1.128		1
451.....	453.31	220.86	16.992		2.432		1
452.....	371.77	231.52	16.873		1.051		1
453.....	123.19	234.25	17.866		2.118		1
454.....	445.45	244.63	16.976		1.154		1
455.....	150.00	251.06	16.562		1.204		1
456.....	137.54	259.73	15.207		0.771		1
457.....	171.20	277.29	16.832		1.279		1
458.....	243.77	277.96	17.007		1.175		1
459.....	305.49	290.49	17.405		1.300		1
460.....	212.12	296.93	16.422		0.910		1
461.....	442.92	299.39	17.060		1.052		1
462.....	279.06	305.78	16.715		1.126		1
463.....	482.38	311.59	16.404		0.895		1
464.....	224.29	312.30	17.032		1.024		1
465.....	397.99	312.83	17.067		2.521		1
466.....	147.33	319.60	17.726		1.744		1
467.....	329.31	342.93	16.846		1.049		1
468.....	214.52	344.47	16.053		0.979		1
469.....	210.07	354.91	16.913		0.876		1
470.....	21.35	357.60	16.279		0.792		1
471.....	206.01	370.55	17.633		1.621		1
472.....	254.74	404.67	16.855		1.055		1
473.....	160.80	405.34	18.151		0.965		1
474.....	2.97	408.42	16.875		2.493		1
475.....	78.13	410.95	17.679		1.158		1
476.....	166.96	413.97	18.071		1.246		1
477.....	143.27	418.78	17.200		1.235		1
478.....	250.71	427.21	15.686		1.098		1
479.....	104.62	432.09	16.915		1.562		1
480.....	287.68	435.57	18.074		1.321		1
481.....	97.85	459.13	16.867		1.151		1
482.....	368.15	482.90	18.060		1.112		1
483.....	458.07	488.87	15.295		1.496		1
484.....	489.10	495.98	17.463		0.997		1
485.....	424.57	503.37	16.712		2.017		1
486.....	464.70	505.34	16.800		1.316		1
487.....	89.99	505.69	17.769		2.056		1
488.....	170.23	507.30	16.176		0.944		1
489.....	148.92	510.87	14.407		0.572		1
490.....	495.04	15.88	16.702		1.115		1
491.....	268.38	32.71	17.809		2.264		1
492.....	152.13	47.78	17.395		1.123		1
493.....	195.16	65.03	17.217		1.161		1
494.....	153.69	85.45	17.530		1.260		1
495.....	69.55	99.14	16.852		1.579		1
496.....	40.62	106.60	16.914		1.158		1
497.....	330.66	117.78	17.218		1.242		1
498.....	131.83	127.97	17.163		1.897		1
499.....	291.88	131.14	17.342		1.195		1
500.....	202.38	154.07	17.631		1.795		1
501.....	496.98	160.13	17.442		1.163		1
502.....	288.43	258.50	17.460		2.912		1
503.....	12.61	333.70	15.906		1.008		1
504.....	258.06	370.70	16.434		1.064		1
505.....	100.00	384.29	17.062		2.739		1
506.....	93.45	409.41	15.617		0.881		1
507.....	264.35	420.13	16.520		1.882		1
508.....	478.17	470.74	17.312		1.211		1
509.....	396.87	472.47	16.751		0.962		1
510.....	312.18	511.81	18.075		1.213		1
511.....	108.10	17.35	17.357		1.355		1
512.....	34.35	112.09	17.828		3.718		1
513.....	216.02	126.49	16.428		1.056		1
514.....	348.23	317.88	17.305		1.181		1
515.....	296.11	356.75	16.666		1.026		1
516.....	70.27	501.11	16.812		0.881		1
517.....	106.92	250.59	16.221		0.971		1
518.....	133.51	455.67	16.295		0.998		1
519.....	58.85	505.12	16.733		1.975		1
520.....	378.31	456.54	16.500		0.851		1
521.....	409.30	1.72	14.687		0.827		1

TABLE 8

MAGNITUDES AND COLORS OF STARS IN THE FIELD OF NGC 6231

Star	X	Y	V	$\sigma V$	V-I	$\sigma(V-I)$	n
1	217.94	120.87	11.747	0.014	0.385	0.021	3
2	235.60	205.30	12.603	0.061	0.474	0.047	3
3	300.09	159.72	12.704	0.017	1.583	0.027	3
4	199.72	192.59	7.752	0.041	0.281	0.008	3
5	87.25	208.33	12.754	0.021	0.437	0.100	3
6	310.09	213.73	13.010	0.073	2.058	0.077	2
7	312.70	227.66	10.996	0.028	0.351	0.030	3
8	452.54	290.87	9.319	0.039	0.232	0.014	5
9	357.75	350.58	9.422	0.037	0.209	0.029	3
10	259.34	398.77	9.329	0.024	0.219	0.014	3
11	270.42	580.17	12.222		-0.190		1
12	478.22	84.93	12.433	0.124	0.689	0.038	3
13	373.05	87.21	11.465	0.043	0.345	0.056	3
14	520.77	92.16	11.502		0.271		1
15	334.90	127.59	10.078	0.026	0.338	0.036	5
16	112.05	155.42	11.286	0.015	0.317	0.036	3
17	254.04	169.87	8.646	0.031	0.247	0.009	3
18	143.77	233.27	6.330	0.039	0.346	0.007	3
19	422.93	239.48	9.185	0.032	0.267	0.023	5
20	309.83	376.70	11.644	0.027	0.286	0.090	3
21	407.21	397.75	12.048	0.076	1.655	0.039	5
22	539.50	402.06	11.492	0.014	0.342	0.031	2
23	210.53	458.93	12.057	0.073	0.285	0.104	3
24	72.09	192.56	12.249	0.087	0.494	0.060	3
25	99.29	245.51	11.831	0.013	0.347	0.095	3
26	320.57	249.10	10.076	0.057	0.275	0.034	5
27	505.69	524.53	11.606	0.018	0.406	0.042	3
28	212.37	114.37	10.630	0.029	0.334	0.024	3
29	369.17	195.43	11.455	0.028	0.290	0.059	5
30	85.88	347.67	12.127	0.031	0.493	0.067	3
31	135.55	355.24	9.769	0.023	0.253	0.008	3
32	258.64	357.38	9.297	0.022	0.223	0.013	3
33	122.84	358.18	8.602	0.034	0.238	0.014	3
34	453.71	561.30	9.670	0.030	0.260	0.014	3
35	364.54	90.02	12.412	0.065	0.397	0.169	3
36	494.99	479.12	5.334	0.053	0.301	0.027	5
37	134.79	235.78	11.650		-0.530		1
38	341.04	271.75	6.142	0.036	0.273	0.012	5
39	112.67	484.01	10.163	0.006	0.316	0.022	3
40	739.19	622.87	11.536		0.404		1
41	572.85	253.05	10.531	0.016	0.266	0.019	2
42	629.92	450.89	9.195		0.249		1
43	760.66	258.14	13.046		0.686		1
44	342.48	421.18	12.977	0.051	0.409	0.192	3
45	630.45	422.47	11.451		0.220		1
46	619.98	433.68	6.520		0.253		1
47	623.86	475.27	13.060		2.642		1
48	480.75	502.02	12.711		0.583		1
49	642.36	551.51	12.326		0.491		1
50	517.12	622.40	11.859		0.341		1
51	727.05	623.10	11.677		0.556		1
52	677.26	147.51	12.697		0.468		1
53	644.29	268.69	12.779		0.309		1
54	617.86	451.18	9.196		0.268		1
55	630.17	551.55	12.382		0.541		1
56	689.62	211.85	12.510		0.298		1
57	752.65	524.60	12.568		0.334		1
58	504.95	622.72	11.885		0.185		1
59	617.20	419.04	13.482		2.074		1
60	607.90	434.07	6.527		0.264		1
61	126.61	85.35	12.783	0.038	0.557	0.032	2
62	146.54	134.41	13.294	0.026	0.575	0.055	2
63	251.02	187.36	11.921	0.040	0.472	0.060	2
64	152.55	254.73	12.333		0.541		1
65	273.66	271.97	13.405	0.012	0.599	0.081	2
66	273.01	347.27	13.197	0.030	0.771	0.025	2
67	341.40	3.90	11.078	0.037	0.404	0.033	2
68	158.48	11.62	12.475	0.004	0.520	0.036	2
69	246.95	32.06	12.045	0.009	0.357	0.005	2
70	477.45	40.90	12.736	0.005	0.461	0.005	2
71	233.38	67.71	13.021	0.065	0.514	0.082	2
72	407.72	73.21	10.897	0.016	0.336	0.003	2
73	44.45	130.20	13.490	0.064	0.848	0.059	2

TABLE 8—Continued

Star	X	Y	V	$\sigma V$	V-I	$\sigma(V-I)$	n
74	87.93	227.93	13.341		0.658		1
75	352.89	487.98	12.817	0.055	0.458	0.047	2
76	380.35	26.79	6.513	0.018	0.319	0.006	2
77	53.59	64.51	9.526	0.006	0.308	0.002	2
78	249.17	295.53	12.740		0.371		1
79	467.48	444.93	12.712	0.021	0.400	0.042	2
80	349.90	10.16	13.662		0.901		1
81	249.08	24.40	8.149	0.010	0.319	0.001	2
82	24.26	306.64	12.158	0.030	0.629	0.037	2
83	101.64	379.86	12.604	0.029	0.493	0.042	2
84	25.73	449.40	10.826	0.008	0.394	0.006	2
85	392.99	33.78	11.834		0.291		1
86	31.98	301.48	14.187		0.915		1
87	365.42	349.14	14.453		4.975		1
88	332.97	270.64	12.066		0.071		1
89	350.55	350.88	9.398		0.223		1
90	186.50	448.68	13.663		0.797		1

NGC 6231 (5 Myr), while the lower portion was built using the fiducial sequence of NGC 6451 (4 Gyr). The common sections of the unevolved MSs of the remaining templates define the middle empirical ZAMS. The scatter in color resulting from the superposition of the fiducial sequences is  $\sim 0.02$  mag, and the dispersion in  $M_v$  is  $\leq 0.10$  mag. Notice that these values are consistent with the typical errors

TABLE 9

MAGNITUDES AND COLORS OF STARS IN THE FIELD OF NGC 6242

Star	X	Y	V	$\sigma V$	V-I	$\sigma(V-I)$	n
1	529.11	533.49	12.870	0.086	0.574	0.134	2
2	316.92	106.90	11.998	0.045	1.455	0.014	3
3	435.44	166.70	12.497	0.018	0.473	0.082	2
4	403.08	183.25	13.024		0.555		1
5	691.32	201.86	12.807	0.011	1.091	0.025	2
6	812.54	152.97	12.783	0.037	0.881	0.406	2
7	450.22	178.83	13.047	0.054	0.553	0.069	3
8	773.65	214.46	12.201	0.010	0.492	0.031	2
9	343.66	373.43	12.201	0.058	0.421	0.080	4
10	532.29	468.96	10.266	0.023	0.264	0.014	2
11	386.19	508.71	12.602	0.033	0.539	0.007	2
12	589.99	160.02	12.436	0.036	0.382	0.005	2
13	323.62	293.77	9.849	0.055	0.366	0.032	4
14	598.35	396.22	10.155	0.011	0.256	0.011	2
15	418.47	402.91	8.508	0.062	0.315	0.048	4
16	714.30	457.12	9.512	0.002	0.418	0.006	2
17	624.27	451.34	11.696		0.315		1
18	530.13	549.86	10.696	0.003	0.295	0.006	2
19	445.96	137.15	11.723	0.054	0.322	0.008	4
20	629.39	280.43	13.480		0.566		1
21	494.12	465.20	13.308		0.695		1
22	749.75	601.49	11.961		0.321		1
23	381.43	327.82	12.123		0.503		1
24	125.35	438.47	13.268		0.668		1
25	58.79	178.78	13.013		0.834		1
26	91.06	355.15	13.301		0.621		1
27	47.26	45.73	10.998	0.051	0.375	0.007	2
28	126.64	75.18	10.746	0.055	0.437	0.047	2
29	76.22	142.88	12.564	0.036	0.519	0.022	2
30	69.55	186.61	13.912		0.933		1
31	84.27	197.58	12.082		0.599		1
32	227.50	250.70	12.741	0.036	0.491	0.010	2
33	381.76	319.92	12.191	0.058	0.558	0.035	2
34	223.59	362.84	12.590	0.068	0.493	0.016	2
35	243.83	500.21	9.633		0.442		1
36	267.56	65.66	11.894		0.383		1
37	1.22	142.51	10.956	0.039	0.338	0.040	2
38	102.09	224.43	7.098	0.059	1.674	0.061	2
39	232.70	499.48	12.640		0.408		1
40	378.57	81.04	12.743		1.451		1

TABLE 10

MAGNITUDES AND COLORS OF STARS IN THE FIELD OF NGC 6259

Star	X	Y	V	$\sigma V$	V - I	$\sigma(V - I)$	n
1	782.76	379.34	16.058	0.052	1.114	0.056	2
2	550.21	384.99	13.317	0.030	0.806	0.035	2
3	384.83	206.83	15.556	0.050	1.119	0.073	4
4	383.23	246.86	16.133	0.094	1.074	0.117	2
5	567.78	249.97	12.273	0.041	1.725	0.043	2
6	647.35	254.79	14.452	0.058	0.744	0.060	2
7	595.10	255.05	13.180	0.055	0.739	0.053	2
8	665.11	262.58	13.826	0.047	0.791	0.057	2
9	407.18	280.13	13.991	0.024	0.843	0.019	4
10	668.06	290.35	14.160	0.035	1.848	0.036	2
11	592.82	298.96	13.957	0.046	0.742	0.044	2
12	365.51	305.05	14.755	0.033	0.919	0.057	4
13	571.81	334.10	17.087		2.019		1
14	595.55	338.84	17.002		1.573		1
15	497.63	339.30	14.520	0.034	0.867	0.022	3
16	628.80	346.04	14.865	0.070	0.793	0.075	2
17	503.00	362.60	15.631	0.036	1.083	0.053	2
18	650.16	382.29	16.527	0.075	1.158	0.163	2
19	767.56	384.90	12.770	0.038	0.817	0.044	2
20	672.77	405.07	16.540	0.106	1.605	0.100	2
21	709.73	426.33	15.602	0.058	2.161	0.054	2
22	488.24	440.67	15.416	0.027	1.121	0.018	4
23	795.24	450.73	16.059		1.412		1
24	795.15	461.34	12.984	0.043	0.736	0.043	2
25	514.07	471.73	12.140	0.040	0.668	0.042	2
26	532.25	495.46	15.858	0.062	1.319	0.018	2
27	416.79	503.07	15.890	0.058	1.055	0.042	2
28	756.33	514.40	13.911	0.043	1.222	0.034	2
29	631.14	519.32	16.366		1.505		1
30	748.99	542.45	15.942	0.082	1.382	0.105	2
31	384.59	595.54	15.961	0.050	1.049	0.029	2
32	795.64	610.10	16.772	0.095	1.312	0.084	2
33	522.62	620.67	14.907	0.050	1.231	0.049	2
34	725.62	624.47	15.527	0.007	1.183	0.007	2
35	787.14	635.58	16.476		2.181		1
36	664.89	636.74	16.408		1.286		1
37	767.12	664.81	15.084		1.773		1
38	821.24	687.98	16.375	0.071	1.352	0.056	2
39	712.12	691.69	12.640	0.047	1.751	0.043	2
40	733.68	699.55	14.331		2.039		1
41	481.87	197.89	15.382	0.040	1.073	0.048	4
42	348.36	203.94	14.737	0.037	0.878	0.047	4
43	715.17	239.06	15.426	0.069	1.039	0.048	2
44	637.03	247.51	16.720		2.430		1
45	470.94	250.21	13.934	0.031	0.754	0.034	4
46	464.93	260.63	14.677	0.038	0.841	0.045	4
47	552.39	319.93	16.454	0.029	1.518	0.044	2
48	565.91	346.60	12.913	0.044	2.903	0.045	2
49	521.53	351.07	15.071	0.062	1.821	0.070	2
50	793.49	359.53	16.833		1.520		1
51	598.62	362.65	16.037	0.059	1.241	0.032	2
52	533.51	405.03	12.888	0.040	0.739	0.051	2
53	636.54	440.03	13.781	0.050	0.876	0.049	2
54	419.71	452.00	16.463	0.095	1.268	0.091	3
55	360.51	471.29	13.696	0.030	0.673	0.021	4
56	394.34	496.74	14.551	0.028	0.765	0.029	4
57	553.72	520.56	15.553	0.052	1.082	0.041	2
58	493.63	525.19	15.447	0.067	1.151	0.083	2
59	389.92	529.85	15.919		1.101		1
60	547.50	534.49	15.117	0.063	0.890	0.074	2
61	557.65	539.87	15.912	0.094	2.033	0.094	2
62	455.74	541.01	15.880	0.084	1.364	0.077	2
63	432.32	564.98	15.640	0.049	0.970	0.077	2
64	377.72	571.68	13.503	0.049	0.761	0.044	2
65	347.32	604.70	14.813	0.015	1.816	0.013	2
66	556.79	617.60	15.920	0.024	1.317	0.005	2
67	684.36	618.96	14.488	0.033	0.895	0.026	2
68	693.77	642.86	13.597	0.036	1.145	0.026	2
69	370.41	646.22	12.807	0.031	0.723	0.032	2
70	399.06	651.15	15.152	0.049	1.830	0.053	2
71	588.39	659.61	16.027		2.357		1
72	500.73	697.13	12.461	0.045	1.775	0.025	2
73	334.65	234.28	15.189	0.051	0.886	0.060	4
74	804.09	514.48	13.852	0.039	0.668	0.047	2
75	366.09	532.08	13.967	0.040	0.708	0.017	2

TABLE 10—Continued

Star	X	Y	V	$\sigma V$	V - I	$\sigma(V - I)$	n
76	402.97	637.57	13.867	0.046	0.705	0.053	2
77	450.43	297.62	12.573	0.029	0.707	0.028	4
78	696.23	360.68	14.083	0.062	0.650	0.206	2
79	692.57	695.30	16.517		1.710		1
80	699.96	506.19	12.425	0.037	1.795	0.035	2
81	546.19	196.05	16.192		2.290		1
82	639.11	307.85	16.351		1.495		1
83	622.30	214.89	16.019		1.053		1
84	827.58	250.00	16.298		1.444		1
85	519.33	326.50	16.618		1.362		1
86	819.05	348.01	16.695		1.367		1
87	665.52	354.72	15.627		1.896		1
88	754.59	441.86	16.653		1.119		1
89	739.94	463.64	16.277		1.078		1
90	362.83	511.91	16.772		1.508		1
91	520.50	540.68	16.129		1.143		1
92	827.40	557.89	17.247		1.621		1
93	576.02	558.72	16.820		1.387		1
94	400.39	584.18	16.679		1.173		1
95	755.83	589.44	11.796		1.022		1
96	783.90	594.41	15.868		2.103		1
97	512.09	622.34	16.333		1.352		1
98	630.71	621.37	16.680		1.319		1
99	410.67	655.80	16.587		1.102		1
100	693.15	697.32	15.885		0.741		1
101	743.95	243.15	16.402		1.246		1
102	396.91	288.39	16.700	0.031	1.160	0.069	2
103	679.36	305.90	14.536		0.785		1
104	725.54	405.61	13.525		1.024		1
105	571.98	413.41	16.918		1.343		1
106	721.33	445.46	16.988		2.071		1
107	507.45	494.31	13.995		1.644		1
108	475.13	527.69	16.556		1.354		1
109	778.45	555.62	12.313		0.691		1
110	828.21	586.72	13.335		0.666		1
111	611.33	590.34	13.769		0.727		1
112	444.15	628.76	15.373		0.968		1
113	367.56	193.03	12.646	0.019	0.763	0.023	3
114	706.93	277.35	11.952		0.932		1
115	620.26	615.02	12.667		0.821		1
116	534.61	643.96	14.379		0.841		1
117	374.65	88.98	13.979	0.003	0.827	0.012	2
118	217.07	101.94	16.808		1.410		1
119	164.28	193.95	16.851		1.487		1
120	96.81	210.15	16.179		1.258		1
121	131.84	318.65	16.297		1.736		1
122	441.42	16.06	14.289	0.011	0.744	0.005	2
123	453.29	17.92	13.538	0.007	0.658	0.010	2
124	466.22	28.37	12.671	0.007	0.680	0.007	2
125	364.13	32.60	12.853	0.015	0.719	0.006	2
126	201.70	41.18	15.495	0.011	1.002	0.019	2
127	257.87	42.66	16.262	0.056	1.076	0.055	2
128	231.22	54.58	16.137	0.090	1.350	0.102	2
129	445.29	58.59	15.734		1.008		1
130	303.64	61.50	16.455		2.279		1
131	319.63	60.03	15.154	0.013	3.400	0.003	2
132	492.60	73.96	16.479		1.286		1
133	340.14	77.89	16.267	0.038	1.111	0.029	2
134	226.35	83.98	16.603		1.308		1
135	294.32	83.20	16.262	0.085	2.230	0.092	2
136	466.85	89.79	16.734		1.440		1
137	167.56	104.30	15.521	0.018	2.204	0.018	2
138	312.23	161.20	16.668		1.396		1
139	358.81	173.66	15.025	0.013	0.907	0.020	2
140	209.77	198.60	15.307	0.018	1.017	0.008	2
141	354.43	205.87	16.694		1.508		1
142	321.20	217.48	15.500	0.007	3.855	0.020	2
143	104.36	225.74	15.163	0.016	0.928	0.007	2
144	201.85	247.43	16.106		1.066		1
145	291.12	256.64	16.844		1.453		1
146	223.75	336.81	16.053		1.003		1
147	99.18	341.45	15.913		1.068		1
148	80.99	366.40	17.218		1.471		1
149	221.43	376.49	15.713	0.052	1.106	0.054	2
150	238.59	385.65	14.003	0.010	0.738	0.004	2
151	173.26	395.07	16.442		1.423		1

TABLE 10—Continued

Star	X	Y	V	$\sigma V$	V - I	$\sigma(V - I)$	n
152.....	283.24	412.83	15.974	0.049	2.917	0.052	2
153.....	323.70	431.00	15.079	0.015	1.023	0.003	2
154.....	20.14	441.31	13.373	0.011	0.814	0.014	2
155.....	453.60	453.46	15.581	0.040	1.029	0.035	2
156.....	300.07	476.12	16.315		1.200		1
157.....	238.73	474.90	15.568	0.008	2.056	0.012	2
158.....	99.10	479.20	13.813	0.004	0.754	0.002	2
159.....	257.65	485.21	16.632		1.982		1
160.....	288.22	490.99	15.627		1.002		1
161.....	242.93	503.26	16.099		1.383		1
162.....	123.13	14.82	14.788	0.011	0.946	0.002	2
163.....	338.27	32.70	12.938	0.015	1.370	0.005	2
164.....	391.59	45.66	15.080		0.806		1
165.....	390.96	53.51	16.161		1.761		1
166.....	353.29	52.83	14.207	0.015	0.788	0.012	2
167.....	99.07	55.05	13.498	0.010	0.720	0.005	2
168.....	79.93	58.95	13.001	0.006	0.719	0.005	2
169.....	349.98	64.38	13.777	0.008	0.766	0.016	2
170.....	246.47	69.64	13.527	0.003	0.732	0.003	2
171.....	15.77	76.94	13.302	0.010	0.686	0.016	2
172.....	87.35	77.57	14.079	0.009	1.713	0.004	2
173.....	115.49	81.84	12.597	0.011	0.855	0.006	2
174.....	73.30	88.62	15.668		3.052		1
175.....	329.14	87.08	15.654	0.004	1.285	0.022	2
176.....	36.34	95.12	16.814		1.199		1
177.....	458.19	133.47	16.062	0.034	1.135	0.079	2
178.....	147.48	134.75	12.657	0.011	1.711	0.007	2
179.....	108.59	138.84	13.761	0.017	0.832	0.009	2
180.....	27.78	139.20	14.768	0.008	0.735	0.020	2
181.....	436.35	170.27	14.261	0.004	0.741	0.009	2
182.....	460.47	174.77	13.422	0.001	0.703	0.009	2
183.....	466.28	181.78	14.198	0.022	0.775	0.002	2
184.....	66.73	190.44	16.466		2.302		1
185.....	64.69	198.00	15.606	0.019	0.939	0.011	2
186.....	189.11	198.34	14.605	0.001	0.780	0.017	2
187.....	113.75	213.81	14.857	0.005	0.841	0.009	2
188.....	172.13	220.61	14.077	0.004	1.045	0.007	2
189.....	196.67	221.18	15.195	0.034	0.860	0.037	2
190.....	44.85	225.31	12.383	0.005	0.794	0.007	2
191.....	257.65	255.36	12.190	0.002	1.792	0.002	2
192.....	31.03	263.64	14.320	0.044	0.675	0.041	2
193.....	32.78	276.46	14.045	0.020	0.791	0.021	2
194.....	273.77	280.27	14.565	0.006	0.941	0.036	2
195.....	291.84	284.55	12.835	0.009	0.803	0.007	2
196.....	171.86	288.28	14.119	0.006	0.818	0.005	2
197.....	327.06	309.08	13.835	0.010	0.866	0.003	2
198.....	120.43	330.66	12.422	0.002	0.613	0.001	2
199.....	167.26	353.41	15.617		0.958		1
200.....	111.41	355.88	12.614	0.009	0.760	0.002	2
201.....	106.06	403.09	14.317	0.009	0.811	0.004	2
202.....	140.05	407.66	14.231	0.005	0.911	0.016	2
203.....	17.82	418.16	15.593	0.047	4.435	0.040	2
204.....	263.32	421.96	13.091	0.011	0.821	0.006	2
205.....	301.60	436.08	16.051		1.235		1
206.....	141.74	447.23	12.787	0.001	1.812	0.006	2
207.....	84.80	453.32	12.635	0.008	0.745	0.001	2
208.....	92.51	459.25	15.227	0.012	0.893	0.019	2
209.....	71.77	462.00	16.320		1.044		1
210.....	188.54	466.79	14.226	0.003	0.814	0.014	2
211.....	188.25	491.08	14.316	0.012	1.848	0.003	2
212.....	17.50	498.54	16.524		1.322		1
213.....	204.04	48.92	15.684	0.009	0.877	0.003	2
214.....	148.12	277.19	14.173	0.014	0.744	0.163	2
215.....	66.75	288.57	15.742	0.019	1.177	0.025	2
216.....	74.11	291.05	16.018	0.115	1.282	0.083	2
217.....	79.24	340.54	14.437	0.017	0.857	0.002	2
218.....	199.05	380.87	15.892		1.092		1
219.....	57.11	474.03	14.541	0.001	0.848	0.130	2
220.....	351.95	103.87	16.732		1.700		1
221.....	97.75	98.14	16.384		1.131		1
222.....	215.59	418.54	16.394		1.178		1
223.....	465.87	119.21	16.864		1.367		1
224.....	490.62	120.74	15.402		0.955		1
225.....	29.06	265.87	15.375		0.907		1
226.....	68.69	470.04	14.972		0.912		1

TABLE 11

MAGNITUDES AND COLORS OF STARS IN THE FIELD OF IC 4651

Star	X	Y	V	$\sigma V$	V - I	$\sigma(V - I)$	n
1.....	844.11	137.92	12.413	0.032	0.594	0.007	2
2.....	696.16	247.77	13.655	0.016	0.890	0.006	2
3.....	506.72	248.77	15.241	0.025	0.937	0.009	2
4.....	914.82	291.27	14.946	0.015	1.101	0.052	2
5.....	652.17	299.42	15.944	0.011	1.031	0.130	2
6.....	878.78	305.80	16.486		1.194		1
7.....	655.97	320.27	15.463	0.008	0.835	0.315	2
8.....	848.80	371.22	16.188		1.402		1
9.....	715.65	448.57	15.566	0.041	0.985	0.034	2
10.....	587.05	518.19	16.526		1.078		1
11.....	707.30	527.21	13.819	0.045	0.745	0.011	2
12.....	707.04	597.92	16.235	0.020	1.034	0.087	2
13.....	900.56	630.52	13.696	0.006	0.715	0.035	2
14.....	521.82	135.35	16.050	0.026	1.607	0.025	2
15.....	862.41	138.32	13.665	0.016	1.094	0.001	2
16.....	509.52	164.59	11.906	0.017	0.762	0.009	2
17.....	942.54	164.78	10.081	0.010	1.217	0.019	2
18.....	575.35	173.95	13.222	0.022	0.686	0.009	2
19.....	868.81	175.11	14.450	0.011	0.766	0.001	2
20.....	595.95	206.99	15.232	0.015	1.170	0.017	2
21.....	561.33	209.57	13.322	0.011	1.183	0.012	2
22.....	561.61	223.71	14.260	0.025	0.978	0.017	2
23.....	517.79	229.31	15.607	0.091	0.903	0.056	2
24.....	796.43	238.47	11.401	0.010	1.206	0.017	2
25.....	869.88	246.16	13.710	0.010	1.979	0.016	2
26.....	583.11	258.21	12.701	0.011	0.631	0.012	2
27.....	542.01	266.36	13.853	0.016	0.712	0.006	2
28.....	527.65	298.13	12.222	0.016	0.629	0.025	2
29.....	580.93	300.59	14.385	0.001	0.848	0.014	2
30.....	488.36	320.19	13.727	0.034	1.240	0.018	4
31.....	859.71	362.10	12.364	0.011	0.601	0.014	2
32.....	652.29	381.46	15.983	0.069	0.884	0.081	2
33.....	906.67	399.24	15.219	0.029	1.421	0.044	2
34.....	622.02	405.58	15.931	0.035	1.324	0.080	2
35.....	810.22	409.39	14.206	0.018	0.744	0.008	2
36.....	923.65	417.61	14.813	0.010	1.311	0.030	2
37.....	861.90	421.08	14.065	0.031	0.869	0.004	2
38.....	879.56	430.48	13.720	0.027	0.748	0.002	2
39.....	857.09	444.49	12.967	0.020	0.425	0.015	2
40.....	834.06	440.85	16.120		1.482		1
41.....	554.18	504.37	14.823	0.042	0.998	0.035	2
42.....	653.22	526.20	15.489		1.047		1
43.....	837.15	539.17	13.823	0.004	1.349	0.021	2
44.....	484.06	552.83	15.764	0.032	1.171	0.092	2
45.....	731.45	562.62	12.786	0.012	0.589	0.014	2
46.....	836.68	562.87	13.791	0.025	1.091	0.004	2
47.....	765.67	565.55	14.895	0.014	0.744	0.041	2
48.....	693.49	568.36	12.986	0.017	0.675	0.010	2
49.....	722.49	613.34	15.710	0.011	1.078	0.037	2
50.....	793.20	623.31	14.262	0.004	1.575	0.030	2
51.....	818.45	180.68	16.269		1.079		1
52.....	456.03	209.40	14.803	0.036	0.786	0.011	4
53.....	513.55	266.49	13.802	0.004	0.723	0.037	2
54.....	919.01	265.40	15.913	0.008	0.955	0.014	2
55.....	504.26	282.73	16.139	0.027	1.144	0.026	2
56.....	554.76	288.11	13.458	0.012	0.722	0.012	2
57.....	468.07	297.04	13.536	0.042	0.673	0.019	4
58.....	808.99	328.97	10.663	0.012	1.084	0.014	2
59.....	471.75	334.49	12.407	0.032	0.621	0.022	4
60.....	679.63	342.58	15.070	0.021	1.351	0.041	2
61.....	709.09	344.87	13.328	0.010	0.619	0.015	2
62.....	695.97	346.25	15.252		0.987		1
63.....	687.33	353.48	12.072	0.011	0.623	0.007	2
64.....	557.04	368.88	11.830	0.011	0.669	0.011	2
65.....	667.93	369.40	11.608	0.012	0.599	0.007	2
66.....	678.38	374.88	12.035	0.016	0.622	0.009	2
67.....	795.22	370.96	15.413	0.079	0.918	0.004	2
68.....	733.72	389.75	11.869	0.010	0.657	0.016	2
69.....	462.61	408.27	13.289	0.035	1.452	0.024	4
70.....	561.08	412.54	14.336		0.836		1
71.....	462.66	488.07	12.917	0.029	0.654	0.018	4
72.....	625.15	578.94	16.137		1.115		1
73.....	699.79	621.84	10.145	0.007	1.220	0.019	2

TABLE 11—Continued

Star	X	Y	V	$\sigma V$	$V - I$	$\sigma(V - I)$	n
74	516.83	632.09	12.455	0.008	0.596	0.027	2
75	495.32	138.64	12.020	0.042	0.679	0.022	4
76	480.34	201.99	11.990	0.036	0.671	0.019	4
77	587.52	322.12	12.734	0.018	0.612	0.006	2
78	829.50	450.09	14.321	0.026	0.752	0.048	2
79	492.72	573.28	10.616	0.009	1.156	0.015	2
80	506.17	260.84	12.886	0.016	0.603	0.012	3
81	736.34	375.74	14.692	0.055	1.491	0.034	2
82	665.25	614.69	11.869	0.017	0.652	0.005	2
83	566.34	546.76	12.712	0.015	0.594	0.011	2
84	552.24	569.33	13.028	0.010	0.667	0.017	2
85	615.97	433.74	15.927	0.040	0.953	0.040	2
86	453.46	632.34	13.871	0.019	0.687	0.032	2
87	553.18	163.98	16.730		1.021		1
88	849.46	379.38	16.233		1.415		1
89	904.56	493.27	16.082		1.138		1
90	680.24	141.99	16.025		0.977		1
91	861.90	170.43	16.664		1.404		1
92	762.61	204.25	15.948		1.327		1
93	840.17	287.54	15.024		0.934		1
94	862.46	289.31	15.568		1.268		1
95	927.17	336.13	15.523		0.965		1
96	578.44	351.33	15.552		1.084		1
97	524.47	485.00	15.963		1.113		1
98	864.13	502.62	15.199		0.966		1
99	721.71	519.04	16.375		1.180		1
100	466.02	194.43	15.066		1.283		1
101	534.75	298.56	13.939		0.658		1
102	792.41	530.18	15.178		0.912		1
103	447.12	578.93	14.823		0.906		1
104	709.26	636.11	13.780		1.100		1
105	820.49	337.67	15.494		1.155		1
106	709.97	514.05	16.046		1.236		1
107	335.67	70.69	16.020		1.172		1
108	411.02	181.39	16.497		1.363		1
109	481.42	227.15	17.112		1.082		1
110	256.96	27.69	12.043	0.015	0.702	0.008	2
111	479.06	32.46	15.925	0.020	1.222	0.076	2
112	168.39	40.75	15.403	0.029	1.009	0.011	2
113	254.51	48.56	15.427	0.024	0.902	0.019	2
114	31.36	135.89	15.122	0.045	1.065	0.018	2
115	431.21	140.37	13.040	0.023	1.316	0.011	2
116	129.76	161.37	15.392	0.066	1.171	0.068	2
117	52.42	165.28	15.545	0.076	1.209	0.039	2
118	465.87	188.61	15.081	0.046	1.306	0.037	2
119	89.21	190.36	15.259	0.023	1.438	0.021	2
120	309.09	222.88	15.969	0.041	1.142	0.036	2
121	354.73	270.13	10.741	0.018	1.132	0.006	2
122	377.37	292.95	15.139	0.010	1.064	0.010	2
123	70.17	317.97	15.234	0.029	1.387	0.019	2
124	322.96	325.78	13.984	0.020	1.520	0.022	2
125	146.13	339.10	14.736	0.082	1.474	0.073	2
126	358.02	344.39	16.016	0.059	1.063	0.059	2
127	433.23	357.27	16.531		1.198		1
128	347.21	473.97	14.732	0.003	2.667	0.005	2
129	259.83	483.93	16.364		1.444		1
130	384.78	11.59	15.803		1.262		1
131	463.56	33.47	13.812	0.017	0.774	0.001	2
132	50.62	72.47	15.725	0.043	1.064	0.021	2
133	308.65	134.94	12.247	0.021	0.378	0.012	2
134	174.98	135.17	14.726	0.031	1.063	0.028	2
135	201.06	166.67	15.103	0.032	0.951	0.024	2
136	228.03	187.01	12.973		0.680		1
137	373.25	238.41	12.723	0.020	0.663	0.012	2
138	258.46	241.21	13.786	0.022	0.708	0.027	2
139	424.66	256.81	10.729	0.016	1.198	0.007	2
140	368.41	279.17	14.965	0.034	1.374	0.030	2
141	176.17	319.18	13.446	0.037	0.684	0.034	2
142	257.10	364.69	13.580	0.023	0.698	0.017	2
143	178.65	377.34	15.427	0.003	1.042	0.016	2
144	30.03	402.60	13.964	0.014	2.367	0.007	2
145	284.98	437.24	13.392	0.027	1.507	0.016	2
146	189.22	460.57	16.256	0.052	1.058	0.071	2
147	136.54	111.27	13.860	0.040	0.747	0.025	2
148	78.60	322.95	12.657	0.015	0.683	0.008	2

TABLE 11—Continued

Star	X	Y	V	$\sigma V$	$V - I$	$\sigma(V - I)$	n
149	266.57	338.92	12.167	0.021	0.685	0.012	2
150	325.93	6.49	12.234	0.015	0.662	0.013	2
151	171.29	238.87	11.885	0.027	0.573	0.069	2
152	50.90	451.94	15.589		0.984		1
153	20.40	222.49	16.697	0.123	1.502	0.103	2
154	53.77	228.18	11.641	0.023	0.708	0.015	2
155	130.28	446.03	10.180	0.024	1.108	0.014	2
156	37.56	94.16	16.415	0.027	1.354	0.050	2
157	37.10	98.02	17.227		1.492		1
158	145.25	445.38	16.598		3.097		1
159	482.63	419.73	16.652		1.270		1
160	312.61	11.93	16.246		0.955		1
161	6.34	17.30	16.370		1.384		1
162	268.96	107.29	15.773		0.641		1
163	84.34	443.38	16.609		1.167		1
164	165.26	449.66	16.007		1.140		1
165	504.40	52.98	15.573		1.120		1
166	354.81	79.09	15.789		1.245		1
167	413.97	93.99	13.810		1.668		1
168	126.58	147.02	15.104		1.025		1
169	408.26	187.61	16.599		1.479		1
170	271.81	214.77	15.480		0.918		1
171	504.02	282.83	16.249		1.274		1
172	95.18	296.70	15.849		1.155		1
173	234.07	350.15	16.469		1.077		1
174	406.91	465.37	13.437		0.784		1
175	249.10	105.81	16.770		1.221		1
176	359.65	203.79	15.623		1.032		1
177	323.02	249.14	17.284		1.222		1
178	145.73	454.51	14.364		0.867		1

obtained in the determination of the color excess and distance modulus, respectively. Figure 2 shows the empirical ZAMS obtained in the present work (*solid line*) together with those derived by Walker (1985a) (*dotted line*) and Straizys (1990) (*dashed line*), respectively. Our ZAMS presents an excellent agreement with that of Walker along the common color range, so that no zero-point corrections are necessary. The ZAMS of Straizys extends to fainter magnitudes than that of Walker, and, although the agreement seems to be somewhat poorer, it still fits well the lower portion of the ZAMS. The fiducial points of the empirical ZAMS in the  $M_v$  versus  $(V - I)_0$  plane are given in Table 15. Then, we combined the evolved portions of the fiducial sequences for clusters with nearly similar age. To define the empirical 2 Gyr isochrone, the fiducial sequences of NGC 3680 and IC 4651 were averaged; the 200 Myr isochrone was derived from averaging the sequences of NGC 6067 and NGC 6259, and the 50 Myr isochrone was traced by averaging the corresponding curves of NGC 3766 and NGC 6242. The empirical isochrones of 5, 100, 600, and 4000 Myr correspond to the fiducial curves of NGC 6231, NGC 6025, NGC 6633, and NGC 6451, respectively. Figure 3 shows the resulting calibration of the  $M_v$  versus  $(V - I)_0$  diagram as a function of age. We have also included the positions of the giant clumps of NGC 3680 (*squares*), NGC 6067 (*dots*), NGC 6259 (*plus signs*), and IC 4651 (*asterisks*). Table 16 lists the fiducial points of the empirical isochrones in the  $M_v$  versus  $(V - I)_0$  plane. They correspond to the evolved parts of the curves, the ZAMS being excluded.

4. COMPARISON WITH THEORETICAL ISOCHRONES

Theoretical isochrones computed from stellar evolutionary models have long been used to determine basic parameters of Galactic open clusters. In particular, the

TABLE 12

MAGNITUDES AND COLORS OF STARS IN THE FIELD OF NGC 6451

Star	X	Y	V	$\sigma V$	V - I	$\sigma(V - I)$	n
1	224.06	13.77	15.123	0.033	1.148	0.047	3
2	165.90	17.40	14.601	0.024	0.917	0.002	3
3	400.82	24.59	15.387	0.031	2.111	0.007	3
4	373.80	31.67	15.835	0.071	2.411	0.045	3
5	432.00	31.71	12.341	0.005	1.610	0.008	3
6	391.00	38.42	13.671	0.022	0.832	0.014	3
7	289.03	54.50	16.095	0.022	1.843	0.025	3
8	267.37	55.41	15.922	0.038	1.452	0.046	3
9	67.95	59.18	15.952	0.084	1.863	0.039	3
10	329.73	61.11	15.379	0.035	1.301	0.011	3
11	406.88	74.53	13.872	0.051	1.230	0.040	3
12	50.89	75.19	15.585	0.135	1.421	0.093	3
13	239.99	82.65	15.589	0.066	1.384	0.070	3
14	83.11	83.76	9.858	0.008	0.404	0.010	3
15	105.20	92.12	11.206	0.004	0.714	0.016	3
16	178.94	96.71	10.785	0.006	1.651	0.012	3
17	262.09	110.56	15.600	0.041	1.287	0.035	3
18	326.25	125.72	15.090	0.008	2.443	0.021	3
19	137.36	140.06	15.925	0.075	1.240	0.027	3
20	424.94	142.98	13.734	0.018	0.773	0.002	3
21	465.78	143.24	15.774	0.031	1.391	0.046	3
22	113.09	148.99	14.716	0.030	1.207	0.018	3
23	238.01	149.52	12.049	0.008	0.799	0.009	3
24	471.08	163.81	13.815	0.024	1.732	0.010	3
25	82.22	163.94	12.426	0.002	1.030	0.016	3
26	332.63	178.96	12.618	0.006	0.694	0.015	3
27	382.00	189.05	16.383	0.029	4.333	0.013	3
28	497.35	214.14	14.878	0.005	2.098	0.009	3
29	132.81	214.99	12.370	0.006	0.758	0.003	3
30	452.11	218.16	14.497	0.030	1.108	0.016	3
31	150.25	219.94	12.229	0.001	1.582	0.016	3
32	197.68	222.83	15.505	0.016	1.703	0.011	3
33	66.85	228.29	13.964	0.009	0.882	0.011	3
34	275.83	279.45	15.476	0.021	1.114	0.021	3
35	387.91	281.84	14.227	0.029	0.880	0.006	3
36	481.68	285.64	15.737	0.035	1.133	0.024	3
37	396.28	298.13	15.539	0.061	1.338	0.086	3
38	342.44	298.97	12.124	0.007	0.716	0.013	3
39	136.92	305.55	14.119	0.011	0.762	0.057	3
40	300.98	308.31	12.179	0.006	0.816	0.008	3
41	185.70	311.32	15.324	0.053	0.975	0.015	3
42	270.94	317.68	14.036	0.025	1.618	0.004	3
43	79.34	318.07	13.461	0.020	1.159	0.009	3
44	427.55	318.72	14.531	0.011	1.153	0.004	3
45	94.28	324.53	12.359	0.009	0.799	0.010	3
46	306.08	328.29	13.909	0.009	0.840	0.009	3
47	142.09	331.12	14.801	0.014	1.034	0.039	3
48	250.76	333.28	13.605	0.014	0.815	0.002	3
49	373.89	333.50	11.361	0.004	0.813	0.011	3
50	266.52	340.64	12.817	0.018	0.832	0.003	3
51	224.60	343.55	16.453	0.133	1.518	0.090	3
52	164.52	345.22	14.965	0.036	1.117	0.007	3
53	133.99	355.36	14.998	0.030	1.142	0.045	3
54	467.73	360.75	11.193	0.003	0.705	0.011	3
55	42.32	364.39	14.529	0.010	1.192	0.008	3
56	392.61	364.90	14.700	0.036	0.924	0.017	3
57	217.02	366.37	12.396	0.003	0.779	0.023	3
58	281.01	390.87	15.156	0.010	0.982	0.036	3
59	74.87	393.44	12.372	0.010	0.753	0.003	3
60	268.62	393.56	14.067	0.003	0.806	0.034	3
61	261.73	397.36	15.624	0.040	1.198	0.197	3
62	472.03	412.81	14.445	0.015	0.925	0.021	3
63	129.79	414.02	15.879	0.033	1.260	0.042	3
64	457.28	414.50	15.676	0.087	3.140	0.066	3
65	256.76	420.79	15.631	0.039	1.286	0.031	3
66	26.67	428.49	15.301	0.065	1.133	0.022	3
67	458.81	430.44	15.197	0.030	1.384	0.042	3
68	263.64	430.89	14.030	0.012	0.910	0.009	3
69	331.03	458.21	13.937	0.008	0.887	0.032	3
70	413.69	474.09	16.181	0.167	1.358	0.145	3
71	405.00	478.18	12.626	0.008	1.353	0.012	3
72	24.82	478.50	13.341	0.018	0.874	0.007	3
73	361.68	490.96	15.060	0.016	1.477	0.009	3

TABLE 12—Continued

Star	X	Y	V	$\sigma V$	V - I	$\sigma(V - I)$	n
74	172.02	499.20	12.683	0.009	0.794	0.009	3
75	406.79	499.38	13.784	0.008	0.810	0.002	3
76	485.60	21.31	14.288	0.036	1.160	0.034	3
77	490.60	22.51	14.253	0.018	0.941	0.027	3
78	285.00	24.42	15.810	0.038	1.576	0.005	3
79	92.72	42.80	13.286	0.011	1.556	0.010	3
80	95.45	54.86	13.272	0.008	1.014	0.014	3
81	392.71	55.76	13.695	0.018	3.927	0.007	3
82	285.28	73.48	15.038	0.037	1.295	0.077	3
83	344.73	75.04	15.953	0.043	3.361	0.021	3
84	331.75	81.60	16.192	0.068	2.936	0.037	3
85	189.36	89.05	14.519	0.020	1.580	0.034	3
86	388.37	91.52	11.959	0.005	0.720	0.004	3
87	225.86	107.39	15.716	0.043	1.289	0.026	3
88	74.21	108.11	13.914	0.008	0.861	0.027	3
89	252.20	111.59	11.483	0.009	0.839	0.014	3
90	64.21	114.81	15.475	0.066	2.056	0.054	3
91	440.57	115.19	14.259	0.020	1.121	0.012	3
92	162.22	139.76	13.079	0.019	2.829	0.044	3
93	86.03	142.70	15.316	0.026	1.097	0.011	3
94	32.26	143.64	15.266	0.029	1.054	0.016	3
95	9.37	152.76	10.304	0.003	0.661	0.023	2
96	320.58	156.04	13.287	0.006	1.314	0.016	3
97	362.68	156.19	15.314	0.038	0.976	0.020	3
98	10.03	164.97	14.113	0.054	1.012	0.032	3
99	309.02	166.80	14.855	0.013	2.257	0.029	3
100	290.66	167.68	15.434	0.045	1.086	0.045	3
101	497.21	171.50	10.820	0.005	0.743	0.015	3
102	313.18	173.76	12.676	0.005	1.025	0.019	3
103	280.83	176.35	12.286	0.011	0.780	0.002	3
104	369.35	179.39	12.359	0.008	0.758	0.030	3
105	138.59	181.97	15.278	0.020	1.056	0.010	3
106	131.60	184.29	13.763	0.024	1.182	0.025	3
107	426.42	185.04	13.132	0.011	0.802	0.008	3
108	211.10	186.19	15.377	0.044	1.102	0.017	3
109	143.50	205.03	14.388	0.014	0.884	0.026	3
110	210.79	210.54	12.784	0.009	0.721	0.034	3
111	177.88	228.99	14.758	0.026	0.956	0.014	3
112	120.18	232.93	13.449	0.009	0.826	0.011	3
113	149.07	234.42	14.632	0.023	1.056	0.001	3
114	157.63	239.79	14.115	0.009	0.933	0.018	3
115	382.05	243.27	14.219	0.018	1.883	0.003	3
116	167.55	246.24	15.975	0.076	1.696	0.084	3
117	491.65	247.16	14.935	0.034	1.752	0.013	3
118	257.75	249.19	14.515	0.012	0.952	0.039	3
119	344.71	252.36	14.146	0.022	0.943	0.007	3
120	134.56	264.64	15.707	0.065	1.277	0.032	3
121	55.88	287.98	14.788	0.009	1.130	0.016	3
122	122.02	289.28	14.757	0.022	1.114	0.018	3
123	361.78	291.63	16.482	0.028	2.233	0.035	3
124	499.22	293.38	15.800	0.076	1.301	0.064	3
125	231.24	297.74	13.962	0.011	0.793	0.012	3
126	274.78	306.21	12.927	0.015	0.764	0.007	3
127	243.98	308.06	15.535	0.069	1.241	0.114	3
128	212.88	312.30	14.421	0.018	0.918	0.013	3
129	461.91	313.51	12.359	0.008	0.710	0.012	3
130	167.99	315.33	13.964	0.014	0.857	0.023	3
131	136.25	323.40	15.079	0.034	1.296	0.026	3
132	169.60	330.43	13.669	0.009	0.836	0.037	3
133	179.67	332.48	13.843	0.014	0.945	0.028	3
134	453.51	347.61	14.498	0.015	1.292	0.010	3
135	380.55	347.81	12.252	0.007	1.239	0.008	3
136	426.60	351.03	15.474	0.020	1.211	0.021	3
137	108.15	351.35	12.506	0.004	0.892	0.022	3
138	315.07	353.45	15.124	0.012	1.344	0.046	3
139	36.87	355.93	15.716	0.024	1.990	0.013	3
140	242.72	357.48	15.724	0.030	1.316	0.032	3
141	377.17	362.29	15.165	0.058	2.202	0.032	3
142	155.08	367.18	12.060	0.007	0.837	0.009	3
143	340.85	375.68	12.785	0.005	0.829	0.018	3
144	8.62	378.08	12.297	0.004	0.832	0.001	3
145	113.93	388.78	12.086	0.011	0.832	0.011	3
146	320.54	390.21	10.574	0.007	1.454	0.009	3
147	462.38	393.18	14.641	0.018	1.081	0.013	3

TABLE 12—Continued

Star	X	Y	V	$\sigma V$	V - I	$\sigma(V - I)$	n
148.....	189.45	399.39	15.461	0.046	1.331	0.017	3
149.....	323.58	402.54	15.383	0.036	1.237	0.058	3
150.....	467.19	417.37	14.850	0.021	0.901	0.016	3
151.....	276.98	424.40	15.326	0.022	1.320	0.024	3
152.....	98.90	426.24	14.999	0.018	1.130	0.023	3
153.....	294.73	426.51	14.957	0.022	0.976	0.036	3
154.....	299.04	429.43	15.923	0.036	2.093	0.007	3
155.....	423.77	427.86	14.386	0.015	0.889	0.020	3
156.....	137.96	432.64	13.485	0.002	1.754	0.009	3
157.....	180.80	439.39	13.250	0.004	1.164	0.001	3
158.....	186.35	440.63	14.765	0.051	0.933	0.037	3
159.....	151.89	440.32	10.282	0.004	2.274	0.003	2
160.....	299.04	441.95	11.483	0.003	0.542	0.021	3
161.....	18.15	442.25	13.010	0.007	0.789	0.019	3
162.....	340.99	448.70	14.895	0.025	1.235	0.003	3
163.....	308.73	453.18	15.524	0.045	1.252	0.005	3
164.....	227.86	455.02	13.954	0.003	0.837	0.005	3
165.....	279.98	458.33	13.673	0.013	0.832	0.019	3
166.....	110.85	467.25	10.788	0.003	1.707	0.016	3
167.....	318.52	472.24	13.912	0.009	0.979	0.054	3
168.....	444.70	480.25	16.033	0.105	1.631	0.112	3
169.....	299.54	484.53	10.282	0.003	2.321	0.034	2
170.....	213.03	491.25	16.028	0.053	1.346	0.045	3
171.....	160.67	491.33	14.387	0.002	0.898	0.008	3
172.....	492.04	5.68	13.899	0.021	1.019	0.008	3
173.....	56.37	25.88	14.888	0.023	2.037	0.026	3
174.....	298.81	85.30	15.065	0.029	2.071	0.022	3
175.....	346.07	89.79	14.031	0.025	0.856	0.016	3
176.....	315.17	140.60	12.201	0.008	4.586	0.052	3
177.....	59.67	155.62	15.561	0.003	1.102	0.017	3
178.....	77.17	180.87	15.969	0.160	1.552	0.161	3
179.....	392.38	196.19	14.743	0.011	1.058	0.034	3
180.....	121.12	200.41	13.030	0.011	0.789	0.003	3
181.....	124.27	259.20	15.203	0.038	1.079	0.015	3
182.....	379.41	311.33	15.440	0.040	1.066	0.015	3
183.....	5.01	311.35	14.791	0.020	1.089	0.032	3
184.....	24.30	325.36	15.284	0.039	2.213	0.016	3
185.....	405.46	327.44	14.736	0.019	1.131	0.038	3
186.....	424.79	333.66	12.461	0.011	0.770	0.014	3
187.....	419.11	335.90	15.282	0.026	1.615	0.012	2
188.....	198.55	341.27	14.357	0.010	0.855	0.045	3
189.....	258.33	342.44	15.849	0.056	1.389	0.052	3
190.....	324.26	347.26	12.278	0.009	0.707	0.005	3
191.....	235.79	358.35	15.662	0.005	1.308	0.035	3
192.....	300.49	379.43	14.928	0.013	1.525	0.026	3
193.....	465.72	399.53	14.534	0.032	0.825	0.015	3
194.....	198.87	427.63	14.022	0.036	1.060	0.020	3
195.....	5.28	446.86	13.388	0.008	1.666	0.014	3
196.....	258.33	455.58	14.804	0.058	1.433	0.338	3
197.....	103.62	458.74	15.872	0.140	1.250	0.046	3
198.....	470.35	461.75	16.105	0.021	1.347	0.028	3
199.....	271.46	469.86	12.994	0.005	0.803	0.024	3
200.....	303.36	105.28	15.797	0.126	1.451	0.102	3
201.....	318.26	169.47	12.125	0.009	0.825	0.009	3
202.....	305.21	478.68	14.727		1.034		1
203.....	183.39	106.83	14.628	0.032	1.272	0.053	3
204.....	302.73	3.37	16.569	0.018	1.683	0.033	2
205.....	67.21	4.18	17.691	0.035	3.807	0.047	2
206.....	484.19	12.68	17.504	0.010	3.924	0.017	2
207.....	239.06	13.31	16.645	0.020	3.217	0.029	2
208.....	472.27	18.14	16.699	0.008	1.427	0.075	2
209.....	369.92	18.27	17.987	0.040	3.937	0.036	2
210.....	4.81	18.40	15.810	0.009	1.523	0.025	2
211.....	84.43	20.28	18.148		1.536		1
212.....	272.27	22.48	17.982		4.056		1
213.....	292.95	22.68	18.293		4.018		1
214.....	167.18	25.80	17.930		1.970		1
215.....	376.50	39.86	15.969	0.000	1.206	0.029	2
216.....	368.18	43.06	16.093		1.271		1
217.....	347.69	43.11	16.528	0.018	1.358	0.003	2
218.....	209.19	43.61	17.724		2.907		1
219.....	71.38	43.94	18.079		1.490		1
220.....	183.54	45.11	17.828		1.657		1
221.....	212.32	49.87	17.340		1.580		1
222.....	83.89	52.65	16.582	0.046	4.003	0.042	2

TABLE 12—Continued

Star	X	Y	V	$\sigma V$	V - I	$\sigma(V - I)$	n
223.....	162.78	53.11	16.655	0.034	1.449	0.034	2
224.....	31.66	54.29	16.879	0.059	1.326	0.050	2
225.....	487.91	60.29	17.725	0.033	3.505	0.029	2
226.....	297.45	66.28	17.473	0.066	3.309	0.056	2
227.....	153.41	66.37	17.548		1.712		1
228.....	304.79	67.61	17.829		3.066		1
229.....	66.28	72.01	16.821	0.030	2.749	0.025	2
230.....	381.91	75.71	16.401	0.005	1.414	0.000	2
231.....	389.76	78.05	17.483		1.517		1
232.....	438.57	78.54	17.411	0.002	3.684	0.002	2
233.....	231.80	79.20	17.154	0.025	1.479	0.008	2
234.....	18.06	80.01	16.796	0.003	1.383	0.086	2
235.....	313.72	80.49	18.434		4.850		1
236.....	201.71	84.60	16.735	0.006	1.672	0.000	2
237.....	33.29	85.34	17.754		1.943		1
238.....	133.80	87.51	17.641		4.050		1
239.....	284.81	88.76	17.174	0.014	1.444	0.039	2
240.....	55.43	97.51	17.004	0.047	4.078	0.042	2
241.....	491.43	94.30	17.449		1.459		1
242.....	7.62	100.36	16.951	0.031	1.240	0.020	2
243.....	140.77	103.85	17.933		3.114		1
244.....	481.50	104.97	18.055		2.929		1
245.....	48.50	106.84	15.882	0.003	1.129	0.012	2
246.....	165.25	115.94	17.168	0.026	1.866	0.037	2
247.....	120.37	124.66	17.720		3.885		1
248.....	351.63	130.27	16.362	0.002	1.469	0.020	2
249.....	419.54	131.32	18.014		3.075		1
250.....	191.75	132.32	18.020		4.281		1
251.....	187.26	135.33	17.003	0.042	2.822	0.049	2
252.....	248.19	136.08	16.309	0.004	2.737	0.003	2
253.....	222.90	141.03	18.438		1.113		1
254.....	145.11	143.97	17.291	0.028	1.577	0.030	2
255.....	260.37	152.23	16.979	0.030	1.225	0.021	2
256.....	128.99	155.63	16.893	0.014	3.983	0.009	2
257.....	98.26	159.30	16.189	0.009	1.315	0.022	2
258.....	70.15	163.88	15.851	0.023	1.867	0.011	2
259.....	268.24	164.16	17.392		1.219		1
260.....	346.70	164.52	17.316	0.035	4.836	0.034	2
261.....	49.13	171.04	17.914		3.988		1
262.....	219.61	174.01	17.158	0.030	4.797	0.041	2
263.....	209.28	177.35	15.871	0.015	1.264	0.018	2
264.....	55.52	179.82	18.097		3.332		1
265.....	44.10	182.54	16.826	0.031	1.521	0.015	2
266.....	440.89	185.69	17.561	0.015	1.868	0.066	2
267.....	62.74	188.51	18.697		5.299		1
268.....	291.24	192.30	16.915	0.043	1.353	0.016	2
269.....	477.22	201.38	17.710	0.009	1.625	0.008	2
270.....	421.91	204.62	17.798		2.421		1
271.....	494.82	205.24	18.126		2.422		1
272.....	64.43	205.78	17.758		3.607		1
273.....	389.86	207.69	16.299	0.005	1.590	0.020	2
274.....	294.40	213.76	17.151		1.581		1
275.....	89.71	215.84	17.790		1.490		1
276.....	328.41	216.71	17.114		1.313		1
277.....	282.59	219.11	17.435		1.796		1
278.....	270.76	220.55	17.292	0.055	1.694	0.075	2
279.....	434.22	220.93	17.904		3.599		1
280.....	192.29	224.51	17.039		1.349		1
281.....	493.04	225.34	17.411	0.058	3.715	0.045	2
282.....	91.51	230.34	16.283	0.012	2.438	0.009	2
283.....	429.11	231.89	18.042		4.748		1
284.....	168.01	235.75	17.471	0.058	1.964	0.023	2
285.....	367.87	245.89	15.888	0.004	1.151	0.017	2
286.....	4.56	249.90	16.892	0.046	1.396	0.011	2
287.....	437.35	256.18	17.653	0.059	3.005	0.079	2
288.....	103.29	261.41	17.619		1.487		1
289.....	377.26	264.98	17.975	0.038	4.653	0.038	2
290.....	260.26	266.44	17.651	0.013	1.791	0.002	2
291.....	65.92	266.66	17.863	0.055	2.105	0.023	2
292.....	143.69	266.95	17.465	0.059	2.018	0.058	2
293.....	392.05	270.46	16.970	0.028	3.572	0.033	2
294.....	365.59	275.49	17.329	0.015	1.589	0.044	2
295.....	371.44	275.70	17.548	0.031	2.479	0.005	2
296.....	161.87	278.22	18.005		1.914		1
297.....	495.21	281.66	18.043		3.566		1

TABLE 12—Continued

Star	X	Y	V	$\sigma V$	V - I	$\sigma(V - I)$	n
298.....	140.09	284.86	18.552		3.970		1
299.....	341.10	287.04	16.895	0.023	4.740	0.021	2
300.....	285.61	289.81	17.871		3.096		1
301.....	222.59	293.86	15.734	0.015	1.319	0.017	2
302.....	98.02	295.56	16.615	0.007	2.074	0.015	2
303.....	353.70	299.90	16.857	0.027	1.454	0.070	2
304.....	177.71	301.89	17.222	0.017	3.364	0.025	2
305.....	252.98	304.19	17.752		1.258		1
306.....	446.68	304.31	17.915		1.498		1
307.....	258.12	314.95	16.601	0.039	1.283	0.048	2
308.....	480.09	317.64	16.564	0.012	3.687	0.008	2
309.....	231.68	334.52	16.218	0.005	1.503	0.014	2
310.....	473.66	342.14	17.490	0.051	2.451	0.056	2
311.....	352.76	344.52	18.063		3.335		1
312.....	21.76	356.53	17.038	0.056	3.381	0.059	2
313.....	79.32	362.31	17.868		1.694		1
314.....	289.77	370.70	17.365	0.016	5.704	0.013	2
315.....	433.13	372.28	16.826	0.017	1.005	0.055	2
316.....	459.26	373.83	17.239	0.033	2.736	0.049	2
317.....	417.11	374.40	17.161	0.012	1.394	0.023	2
318.....	395.46	374.76	16.580	0.023	3.706	0.025	2
319.....	376.73	381.07	18.010	0.045	3.668	0.041	2
320.....	237.16	384.95	17.117	0.040	1.571	0.003	2
321.....	186.25	387.29	17.609	0.048	3.465	0.051	2
322.....	198.81	389.98	17.100	0.029	4.116	0.029	2
323.....	248.22	393.28	15.947	0.039	1.436	0.011	2
324.....	381.62	393.25	16.187	0.017	1.198	0.008	2
325.....	435.75	398.68	17.924		1.990		1
326.....	24.81	400.16	18.814		3.459		1
327.....	127.14	401.20	17.110		1.306		1
328.....	11.38	402.06	16.681	0.009	1.212	0.050	2
329.....	291.59	414.15	16.389	0.014	1.572	0.015	2
330.....	305.55	414.76	18.315		3.622		1
331.....	7.93	416.03	16.519	0.014	1.538	0.035	2
332.....	118.22	420.10	17.879		3.931		1
333.....	387.03	420.95	15.984	0.023	1.051	0.015	2
334.....	348.99	421.47	17.834		4.558		1
335.....	78.48	422.23	16.238	0.047	1.385	0.090	2
336.....	393.26	424.08	18.570		3.528		1
337.....	343.03	436.94	17.418		1.456		1
338.....	97.50	438.54	18.316		4.011		1
339.....	460.64	438.88	17.233		3.898		1
340.....	112.22	439.81	17.693	0.071	3.591	0.067	2
341.....	3.75	439.90	13.846	0.002	0.863	0.002	2
342.....	428.79	444.42	16.951	0.000	1.661	0.058	2
343.....	455.58	466.59	16.954	0.034	1.465	0.264	2
344.....	446.29	467.04	16.820		1.458		1
345.....	473.90	469.75	17.447		4.217		1
346.....	66.41	470.19	18.107		1.924		1
347.....	378.42	474.91	16.770	0.009	1.520	0.059	2
348.....	496.89	482.16	16.779	0.009	1.238	0.025	2
349.....	125.66	482.66	17.853		1.419		1
350.....	335.21	485.89	16.624	0.005	1.469	0.013	2
351.....	280.08	487.12	17.548		1.505		1
352.....	96.86	487.38	16.726	0.004	2.188	0.026	2
353.....	256.80	487.83	17.404		1.372		1
354.....	393.04	490.66	16.590	0.021	1.147	0.021	2
355.....	404.03	494.34	17.186	0.057	1.657	0.067	2
356.....	280.10	495.45	18.008		1.339		1
357.....	471.54	499.88	17.948		4.898		1
358.....	487.86	500.68	17.147	0.057	2.039	0.001	2
359.....	244.07	503.16	17.526		3.552		1
360.....	256.13	504.41	11.624		0.796		1
361.....	174.69	4.72	17.073		1.686		1
362.....	466.32	5.39	17.529	0.058	1.302	0.027	2
363.....	53.24	7.18	17.425	0.015	1.715	0.044	2
364.....	7.19	9.24	15.943	0.026	1.217	0.038	2
365.....	303.23	13.09	17.632		1.848		1
366.....	344.83	15.16	17.919	0.081	4.082	0.082	2
367.....	19.68	17.10	16.127	0.034	1.382	0.010	2
368.....	217.40	17.51	17.913		1.378		1
369.....	255.50	21.00	17.387		1.480		1
370.....	191.69	22.15	16.733	0.008	1.327	0.015	2
371.....	173.54	22.57	16.610	0.012	1.528	0.036	2
372.....	66.40	23.25	17.946		1.846		1

TABLE 12—Continued

Star	X	Y	V	$\sigma V$	V - I	$\sigma(V - I)$	n
373.....	319.55	26.57	18.108		3.262		1
374.....	100.63	27.18	16.193	0.049	1.354	0.060	2
375.....	325.43	30.81	16.211	0.024	1.383	0.056	2
376.....	260.04	34.20	15.518	0.005	1.343	0.012	2
377.....	289.62	35.54	17.919		3.531		1
378.....	312.39	35.62	16.189	0.021	1.255	0.021	2
379.....	401.39	37.58	17.379	0.052	1.484	0.088	2
380.....	223.57	37.53	17.191	0.026	3.218	0.030	2
381.....	450.39	41.61	18.166		1.398		1
382.....	24.99	44.79	16.965	0.026	1.339	0.041	2
383.....	490.12	44.90	16.245	0.030	1.434	0.004	2
384.....	426.15	45.14	18.825		3.937		1
385.....	153.49	45.31	18.625		5.213		1
386.....	254.74	47.67	17.194	0.024	2.012	0.005	2
387.....	463.80	51.72	16.221	0.017	1.390	0.044	2
388.....	38.85	54.81	16.976	0.030	4.225	0.030	2
389.....	272.63	68.41	16.256	0.010	1.413	0.023	2
390.....	176.86	69.40	17.676	0.089	2.327	0.303	2
391.....	396.64	79.33	16.021	0.010	1.216	0.003	2
392.....	219.45	82.67	17.446	0.046	2.692	0.039	2
393.....	362.17	84.84	17.571		4.192		1
394.....	259.33	89.64	16.617	0.005	3.776	0.013	2
395.....	53.20	93.26	17.379		3.515		1
396.....	201.21	93.74	16.267	0.012	1.610	0.031	2
397.....	457.50	94.06	17.031		3.946		1
398.....	367.81	100.95	16.840	0.031	1.376	0.017	2
399.....	66.32	102.50	17.293	0.002	3.427	0.001	2
400.....	428.25	104.80	16.389	0.023	1.525	0.021	2
401.....	433.39	106.25	17.707	0.084	3.908	0.079	2
402.....	389.72	110.46	16.844	0.001	1.929	0.024	2
403.....	437.66	112.10	17.947		2.458		1
404.....	335.39	112.50	17.240	0.051	4.454	0.048	2
405.....	315.87	116.95	16.116	0.012	1.471	0.016	2
406.....	48.72	120.38	18.114		3.731		1
407.....	471.98	121.15	17.892		3.550		1
408.....	401.50	124.44	15.426	0.025	0.992	0.029	2
409.....	281.97	124.87	17.153	0.070	3.379	0.076	2
410.....	8.25	125.37	17.664	0.028	4.349	0.036	2
411.....	143.00	126.33	16.523	0.022	1.381	0.019	2
412.....	496.81	127.78	17.941	0.125	3.342	0.079	2
413.....	98.86	130.63	18.005	0.026	3.504	0.032	2
414.....	490.71	132.40	17.492	0.048	1.683	0.085	2
415.....	111.03	134.74	17.991	0.079	3.236	0.080	2
416.....	202.63	142.31	18.640		3.341		1
417.....	344.28	144.12	17.670	0.086	3.944	0.083	2
418.....	448.70	144.50	16.541	0.022	1.329	0.093	2
419.....	210.81	151.55	16.976	0.017	2.364	0.008	2
420.....	282.84	155.54	17.681	0.045	4.946	0.043	2
421.....	381.20	155.50	17.715	0.052	4.154	0.051	2
422.....	156.69	158.36	18.229		1.398		1
423.....	215.56	161.84	17.779		1.718		1
424.....	300.84	163.57	16.610	0.018	1.717	0.043	2
425.....	261.89	165.05	17.663	0.059	4.015	0.044	2
426.....	183.91	166.03	17.694	0.037	3.476	0.026	2
427.....	108.24	166.05	16.297	0.008	1.421	0.174	2
428.....	244.29	166.47	18.360		3.535		1
429.....	460.02	167.77	18.046		2.925		1
430.....	157.40	171.41	17.416	0.030	1.966	0.180	2
431.....	456.99	173.41	17.883		2.996		1
432.....	364.72	176.49	16.268	0.030	1.360	0.027	2
433.....	395.72	178.56	17.259	0.035	1.641	0.018	2
434.....	253.36	180.95	17.381	0.057	3.219	0.048	2
435.....	94.18	182.90	17.500		1.531		1
436.....	156.98	183.66	16.051	0.015	1.327	0.004	2
437.....	152.25	183.84	16.447	0.050	1.327	0.067	2
438.....	456.57	184.85	16.505	0.026	1.510	0.061	2
439.....	169.93	187.74	16.956	0.030	1.844	0.011	2
440.....	26.60	188.04	17.132	0.071	3.027	0.083	2
441.....	272.87	190.33	17.090	0.021	4.164	0.026	2
442.....	412.46	192.79	17.186	0.006	1.458	0.029	2
443.....	58.07	194.22	17.617		3.455		1
444.....	442.40	196.55	16.266	0.018	1.240	0.010	2
445.....	31.13	198.95	16.747	0.001	1.292	0.027	2
446.....	380.75	200.96	17.700		1.484		1
447.....	447.45	204.55	16.124	0.008	1.387	0.016	2



TABLE 12—Continued

Star	X	Y	V	$\sigma V$	V - I	$\sigma(V - I)$	n
448.....	280.29	207.45	17.474		1.999		1
449.....	172.35	213.90	17.701	0.092	1.581	0.179	2
450.....	2.42	214.51	18.221		3.549		1
451.....	29.67	215.96	17.327	0.008	1.905	0.036	2
452.....	70.23	216.20	16.814	0.012	2.564	0.011	2
453.....	322.71	220.13	16.938	0.007	2.862	0.029	2
454.....	7.63	223.66	16.533		1.498		1
455.....	502.70	223.98	16.620	0.019	1.525	0.031	2
456.....	170.65	228.08	16.819	0.045	1.521	0.025	2
457.....	353.86	228.70	18.527		3.057		1
458.....	444.81	228.95	17.739		1.935		1
459.....	43.44	236.54	14.755	0.003	1.535	0.023	2
460.....	460.80	237.23	17.922		4.115		1
461.....	5.51	238.20	17.578		1.493		1
462.....	79.75	238.54	16.796	0.021	1.401	0.021	2
463.....	256.80	239.20	16.209		0.171		1
464.....	150.76	242.93	16.363	0.031	2.333	0.039	2
465.....	198.21	244.21	17.644		1.889		1
466.....	227.95	248.96	15.636	0.009	1.404	0.022	2
467.....	431.79	249.05	17.751		3.595		1
468.....	116.00	254.41	16.771	0.021	1.359	0.046	2
469.....	309.53	254.85	17.446	0.052	3.282	0.048	2
470.....	356.15	256.97	17.333	0.035	2.181	0.020	2
471.....	45.14	257.38	17.293		1.074		1
472.....	285.44	257.84	18.160		3.206		1
473.....	366.67	258.88	16.308	0.013	1.424	0.018	2
474.....	463.74	261.00	17.485	0.068	3.499	0.087	2
475.....	191.32	261.05	17.852		3.632		1
476.....	332.35	261.91	17.906		2.380		1
477.....	183.10	261.99	17.399	0.007	1.256	0.396	2
478.....	232.88	264.77	17.239	0.012	2.240	0.013	2
479.....	288.70	265.09	16.464	0.035	1.413	0.051	2
480.....	22.56	267.20	18.220		1.570		1
481.....	87.61	268.06	17.727		3.697		1
482.....	94.45	268.73	17.631		1.758		1
483.....	190.87	271.07	18.231		1.835		1
484.....	305.20	275.07	18.545		4.441		1
485.....	116.44	275.92	17.222	0.064	1.839	0.063	2
486.....	336.31	279.24	16.107	0.007	1.201	0.023	2
487.....	286.52	280.81	17.682		1.435		1
488.....	325.72	282.40	17.826		2.277		1
489.....	111.27	282.47	18.180		4.346		1
490.....	100.43	282.78	18.455		3.955		1
491.....	427.24	283.11	16.929	0.034	1.770	0.240	2
492.....	162.86	289.67	17.989		1.291		1
493.....	174.64	295.17	17.569	0.097	2.163	0.107	2
494.....	405.01	297.49	17.182	0.031	1.700	0.033	2
495.....	195.85	298.26	17.973		1.481		1
496.....	495.71	298.71	18.168		3.831		1
497.....	169.45	300.72	16.380	0.033	1.389	0.004	2
498.....	425.03	305.75	16.945	0.071	4.645	0.065	2
499.....	265.45	308.77	17.946		2.319		1
500.....	89.07	310.09	17.534	0.061	2.486	0.045	2
501.....	71.11	313.48	16.446	0.040	1.457	0.028	2
502.....	56.04	314.46	17.862		1.859		1
503.....	207.09	317.02	17.800		1.542		1
504.....	454.72	323.50	17.669		3.498		1
505.....	132.59	332.55	15.992	0.022	1.485	0.010	2
506.....	72.49	334.42	17.034	0.042	4.352	0.030	2
507.....	112.75	336.94	17.333		1.668		1
508.....	120.83	347.14	17.181	0.031	1.828	0.332	2
509.....	120.88	353.99	17.589	0.047	4.236	0.054	2
510.....	189.07	360.40	15.121	0.001	1.036	0.014	2
511.....	351.13	363.05	18.434		2.523		1
512.....	345.51	368.67	16.868	0.004	0.993	0.030	2
513.....	18.86	370.02	18.010		4.685		1
514.....	368.21	371.74	16.790	0.036	1.711	0.000	2
515.....	489.26	373.01	17.585	0.064	4.677	0.061	2
516.....	187.22	373.16	17.005	0.008	1.734	0.005	2
517.....	309.10	375.29	17.007		1.199		1
518.....	419.46	382.60	18.699		3.257		1
519.....	259.12	383.20	17.466	0.037	2.040	0.026	2
520.....	70.08	384.17	16.502	0.015	1.312	0.029	2
521.....	265.87	384.66	17.017	0.025	1.390	0.000	2
522.....	486.25	390.76	18.550		3.829		1

TABLE 12—Continued

Star	X	Y	V	$\sigma V$	V - I	$\sigma(V - I)$	n
523.....	58.20	392.00	17.255	0.022	2.959	0.017	2
524.....	474.81	396.51	16.619	0.024	1.468	0.022	2
525.....	349.61	398.02	16.357	0.115	2.587	1.512	2
526.....	370.77	401.20	17.903		2.078		1
527.....	460.86	402.40	16.412	0.001	3.868	0.006	2
528.....	184.46	405.80	17.013		1.853		1
529.....	229.55	407.74	15.774	0.010	1.181	0.019	2
530.....	70.88	408.27	17.566	0.028	4.201	0.027	2
531.....	32.69	409.55	17.322	0.019	1.409	0.084	2
532.....	394.18	413.12	17.332		1.249		1
533.....	217.29	421.24	17.086	0.036	4.500	0.038	2
534.....	372.65	422.48	17.905		1.506		1
535.....	416.84	424.59	17.776		1.513		1
536.....	444.20	425.46	16.893	0.016	1.765	0.433	2
537.....	283.41	427.82	17.082	0.061	1.891	0.048	2
538.....	363.49	431.69	16.588	0.036	2.062	0.013	2
539.....	85.13	431.88	17.054	0.027	0.914	0.117	2
540.....	497.66	436.86	16.595	0.006	1.428	0.015	2
541.....	117.78	443.05	16.765	0.058	1.281	0.033	2
542.....	333.59	445.92	16.475	0.017	1.208	0.010	2
543.....	442.55	451.06	16.626	0.053	1.299	0.048	2
544.....	370.12	453.37	17.762		1.469		1
545.....	243.98	457.52	18.391		3.904		1
546.....	201.49	468.47	17.873		4.316		1
547.....	222.71	474.74	17.020	0.061	1.396	0.101	2
548.....	192.00	476.90	17.700	0.043	1.864	0.057	2
549.....	355.68	478.83	15.627	0.010	1.286	0.020	2
550.....	330.48	480.07	16.897		1.460		1
551.....	178.45	481.25	18.473		1.579		1
552.....	349.71	484.59	16.465		1.211		1
553.....	172.12	485.60	17.697		1.439		1
554.....	147.24	486.37	17.417	0.021	1.515	0.110	2
555.....	500.71	490.22	16.576	0.007	1.743	0.059	2
556.....	188.96	491.38	16.454	0.036	1.613	0.049	2
557.....	75.09	494.13	17.727	0.064	5.247	0.058	2
558.....	52.00	494.39	16.691	0.031	1.434	0.040	2
559.....	15.91	503.60	18.232		3.746		1
560.....	87.25	9.88	17.736		2.694		1
561.....	329.35	10.70	17.517	0.018	3.564	0.012	2
562.....	54.29	13.92	17.883		2.512		1
563.....	58.05	16.40	17.516	0.165	3.424	0.135	2
564.....	250.78	34.72	18.041	0.123	2.974	0.132	2
565.....	216.49	35.62	18.073	0.066	3.923	0.055	2
566.....	470.74	45.16	17.172	0.019	3.749	0.015	2
567.....	170.25	45.74	17.504		3.520		1
568.....	366.83	62.49	18.771		3.549		1
569.....	387.53	63.69	16.297	0.019	0.851	0.291	2
570.....	287.96	64.55	18.163		1.967		1
571.....	204.02	65.06	16.823	0.003	2.171	0.013	2
572.....	81.15	68.62	16.555	0.012	2.922	0.003	2
573.....	487.65	74.14	15.844	0.009	1.545	0.013	2
574.....	3.68	89.16	17.887		1.590		1
575.....	269.31	92.45	17.710		2.264		1
576.....	271.85	113.29	17.037	0.005	1.803	0.007	2
577.....	226.04	123.09	17.486		1.575		1
578.....	252.43	125.25	17.487		2.768		1
579.....	297.48	141.58	16.507	0.007	2.077	0.010	2
580.....	212.17	142.47	18.372		3.460		1
581.....	438.30	147.73	19.113		3.592		1
582.....	174.16	149.70	17.957		2.060		1
583.....	485.03	151.91	17.010	0.026	1.657	0.021	2
584.....	71.28	156.54	18.462		2.429		1
585.....	481.35	193.08	17.706		2.140		1
586.....	107.97	200.17	17.873		3.075		1
587.....	227.41	202.88	17.859	0.044	2.145	0.092	2
588.....	192.53	205.42	17.810		3.254		1
589.....	101.35	207.34	17.737		3.294		1
590.....	395.47	209.50	16.073	0.010	1.348	0.027	2
591.....	124.35	215.28	17.461	0.014	3.263	0.003	2
592.....	105.43	226.29	16.439	0.034	1.316	0.034	2
593.....	163.65	224.04	17.654		3.152		1
594.....	164.38	246.74	16.696	0.023	1.195	0.079	2
595.....	476.07	267.78	18.340		3.666		1
596.....	236.96	271.82	17.153	0.004	1.894	0.024	2
597.....	164.09	271.94	17.521		1.515		1

TABLE 12—Continued

Star	X	Y	V	$\sigma V$	V - I	$\sigma(V - I)$	n
598.....	352.46	284.25	17.384		2.175		1
599.....	343.16	311.59	16.413	0.015	1.285	0.031	2
600.....	280.65	319.37	18.073		2.859		1
601.....	275.29	346.33	16.389	0.024	1.273	0.024	2
602.....	266.00	357.53	15.885	0.034	1.155	0.043	2
603.....	165.52	374.78	17.478		3.071		1
604.....	152.12	376.59	16.170	0.028	1.239	0.002	2
605.....	459.62	378.63	16.557	0.012	1.318	0.021	2
606.....	395.70	380.02	18.010		5.639		1
607.....	452.51	382.34	16.539	0.030	1.457	0.018	2
608.....	28.85	383.27	15.311	0.009	1.303	0.049	2
609.....	435.94	383.63	17.584	0.091	2.237	0.115	2
610.....	228.90	400.74	16.747	0.000	1.825	0.008	2
611.....	48.20	405.12	17.846		1.734		1
612.....	125.77	405.87	18.221	0.085	3.237	0.095	2
613.....	353.85	461.35	18.090		3.397		1
614.....	105.05	477.86	16.670		1.435		1
615.....	201.14	486.04	16.428	0.058	3.359	0.045	2
616.....	221.13	490.80	17.519	0.005	3.739	0.006	2
617.....	367.15	496.95	15.740	0.005	1.133	0.015	2
618.....	356.99	498.45	17.728		1.426		1
619.....	123.87	22.94	17.841		2.976		1
620.....	423.91	29.86	16.994	0.029	1.804	0.059	2
621.....	268.38	39.51	17.865		1.416		1
622.....	87.04	46.53	17.107		1.525		1
623.....	103.34	51.70	17.074	0.058	2.757	0.030	2
624.....	37.59	62.69	17.333		1.777		1
625.....	107.19	78.59	16.664		0.925		1
626.....	306.53	90.46	16.846	0.006	2.374	0.329	2
627.....	63.99	94.25	16.587	0.069	1.074	0.076	2
628.....	374.52	141.10	17.490		1.590		1
629.....	92.48	160.71	16.610	0.050	1.365	0.104	2
630.....	502.83	182.82	15.928	0.041	1.178	0.051	2
631.....	234.97	218.90	17.967		3.032		1
632.....	205.16	222.74	17.378	0.001	3.487	0.039	2
633.....	108.71	223.91	16.004	0.007	1.464	0.013	2
634.....	269.14	229.03	16.029		1.795		1
635.....	434.50	232.67	16.670	0.010	2.028	0.000	2
636.....	355.39	240.97	15.839	0.024	1.327	0.051	2
637.....	125.57	241.51	17.283	0.080	3.199	0.071	2
638.....	207.56	286.31	15.250		-0.453		1
639.....	118.88	290.59	16.247	0.019	1.169	0.005	2
640.....	102.67	303.25	17.729		3.210		1
641.....	297.32	313.47	16.094	0.031	3.356	0.026	2
642.....	126.88	384.28	17.598		1.808		1
643.....	465.01	422.18	15.896	0.003	1.413	0.012	2
644.....	329.24	493.62	17.030		1.600		1
645.....	235.39	494.43	16.309		1.286		1
646.....	393.66	95.43	13.898	0.007	0.857	0.005	2
647.....	482.25	156.88	17.447	0.013	2.171	0.020	2
648.....	500.89	191.87	17.504		1.560		1
649.....	352.37	280.20	16.822	0.076	1.830	0.106	2
650.....	472.64	280.07	17.807		3.827		1
651.....	304.31	326.58	16.495	0.005	1.362	0.021	2
652.....	470.09	395.01	16.319	0.027	1.209	0.050	2
653.....	200.64	482.05	16.724	0.009	1.702	0.052	2
654.....	105.71	482.31	17.419		1.762		1
655.....	413.41	136.65	17.954		2.967		1
656.....	80.87	159.68	15.646		2.795		1
657.....	478.51	361.03	16.399	0.095	1.350	0.122	2
658.....	448.82	382.85	16.423	0.012	1.209	0.045	2
659.....	374.99	120.60	18.191		5.273		1
660.....	211.78	289.57	17.149		2.380		1
661.....	66.19	448.39	17.872		5.598		1
662.....	244.70	49.43	17.478		2.580		1
663.....	120.45	101.02	17.536		4.416		1
664.....	16.13	142.63	16.372	0.077	2.169	0.064	2
665.....	459.53	455.70	17.945		2.106		1
666.....	394.92	7.93	17.335		3.424		1
667.....	137.83	44.95	18.158		3.645		1
668.....	88.89	189.64	17.834		3.387		1
669.....	410.13	398.19	17.766		2.560		1
670.....	466.46	500.53	16.229		3.311		1
671.....	238.30	22.84	17.588		3.292		1
672.....	413.94	40.48	18.362		4.617		1

TABLE 12—Continued

Star	X	Y	V	$\sigma V$	V - I	$\sigma(V - I)$	n
673.....	270.28	228.75	17.328		2.976		1
674.....	97.15	312.08	17.417		2.457		1
675.....	399.64	460.86	18.077		3.960		1
676.....	338.09	305.23	16.690		1.192		1
677.....	324.80	502.13	17.951		2.230		1
678.....	109.39	152.92	16.943		4.496		1
679.....	128.49	257.60	16.875		1.416		1
680.....	233.92	494.61	16.761		1.266		1
681.....	358.22	89.92	16.385		3.080		1
682.....	16.02	501.60	17.770		3.368		1
683.....	185.15	102.00	14.504		1.933		1

TABLE 13

MAGNITUDES AND COLORS OF STARS IN THE FIELD OF NGC 6633

Star	X	Y	V	$\sigma V$	V - I	$\sigma(V - I)$	n
1.....	-596.57	877.16	12.264	0.025	0.640	0.025	2
2.....	-394.70	894.63	8.006	0.002	0.285	0.019	2
3.....	-656.51	968.04	13.906	0.023	0.850	0.002	2
4.....	-530.78	1006.42	14.410	0.045	0.891	0.095	2
5.....	-533.91	1081.43	12.413	0.030	1.446	0.018	2
6.....	-294.84	1267.60	12.288	0.003	1.400	0.009	2
7.....	-541.09	1293.37	13.239	0.001	1.526	0.012	2
8.....	-672.06	1325.24	13.958	0.025	0.858	0.006	2
9.....	-344.18	948.90	8.514	0.008	0.386	0.017	2
10.....	-516.80	963.78	14.586	0.080	1.694	0.067	2
11.....	-478.23	1141.59	14.489	0.056	2.023	0.093	2
12.....	-290.16	1179.33	13.740	0.025	0.793	0.060	2
13.....	-585.12	1208.49	7.793	0.008	0.293	0.001	2
14.....	-425.81	1265.49	13.797	0.056	1.486	0.053	2
15.....	-296.26	1202.64	8.424	0.010	0.388	0.007	2
16.....	-292.18	1203.60	6.795	0.001	0.102	0.019	2
17.....	-223.09	1350.92	12.712	0.044	1.220	0.019	2
18.....	-692.58	1218.53	14.604		0.757		1
19.....	-381.82	1074.48	14.675		1.598		1
20.....	487.81	1461.18	14.735		1.095		1
21.....	231.02	1507.84	14.357	0.009	0.849	0.030	2
22.....	1.98	1588.68	14.751		1.307		1
23.....	306.37	1493.27	11.491	0.016	1.835	0.013	2
24.....	53.86	1533.19	15.327		1.382		1
25.....	153.22	1558.78	14.854		1.448		1
26.....	349.33	1587.62	11.055	0.004	1.238	0.015	2
27.....	448.26	1592.30	13.231	0.003	1.898	0.035	2
28.....	329.23	1652.88	8.019	0.001	0.303	0.030	2
29.....	499.31	1747.72	14.811		0.831		1
30.....	297.21	1789.62	13.278	0.012	1.358	0.024	2
31.....	208.58	1795.77	7.303	0.014	1.087	0.001	2
32.....	323.39	1812.25	9.453	0.011	0.275	0.012	2
33.....	132.46	1859.02	9.458	0.012	0.435	0.017	2
34.....	70.21	1912.31	14.297		0.647		1
35.....	342.89	1481.72	12.806	0.005	0.907	0.015	2
36.....	419.51	1571.00	13.575	0.057	2.702	0.051	2
37.....	93.61	1572.79	12.788	0.025	1.518	0.001	2
38.....	79.55	1632.45	13.405	0.032	0.710	0.088	2
39.....	265.67	1750.05	13.863	0.009	0.790	0.048	2
40.....	53.23	1795.73	9.535	0.009	0.415	0.010	2
41.....	70.00	1870.27	12.965	0.011	0.904	0.042	2
42.....	131.34	1940.67	13.656	0.034	1.376	0.051	2
43.....	84.30	1623.79	15.219		1.345		1
44.....	75.33	99.02	13.754	0.045	1.221	0.086	2
45.....	21.69	176.24	14.611		1.380		1
46.....	363.69	227.34	10.289	0.024	0.612	0.024	2
47.....	186.90	296.44	14.279	0.131	1.441	0.094	2
48.....	135.83	38.24	13.745	0.020	0.391	0.113	2
49.....	425.13	215.06	14.383	0.025	1.541	0.039	2
50.....	236.85	271.25	12.285	0.023	0.721	0.057	2
51.....	437.79	304.60	13.778	0.008	1.068	0.002	2
52.....	382.73	406.02	11.123	0.013	0.679	0.025	2
53.....	345.60	440.72	8.637	0.013	0.394	0.003	2
54.....	215.65	176.34	7.488	0.014	0.363	0.017	2
55.....	337.77	343.88	12.908	0.026	0.905	0.058	2
56.....	360.11	286.37	7.653	0.020	0.439	0.019	2
57.....	204.25	375.34	15.026		1.241		1

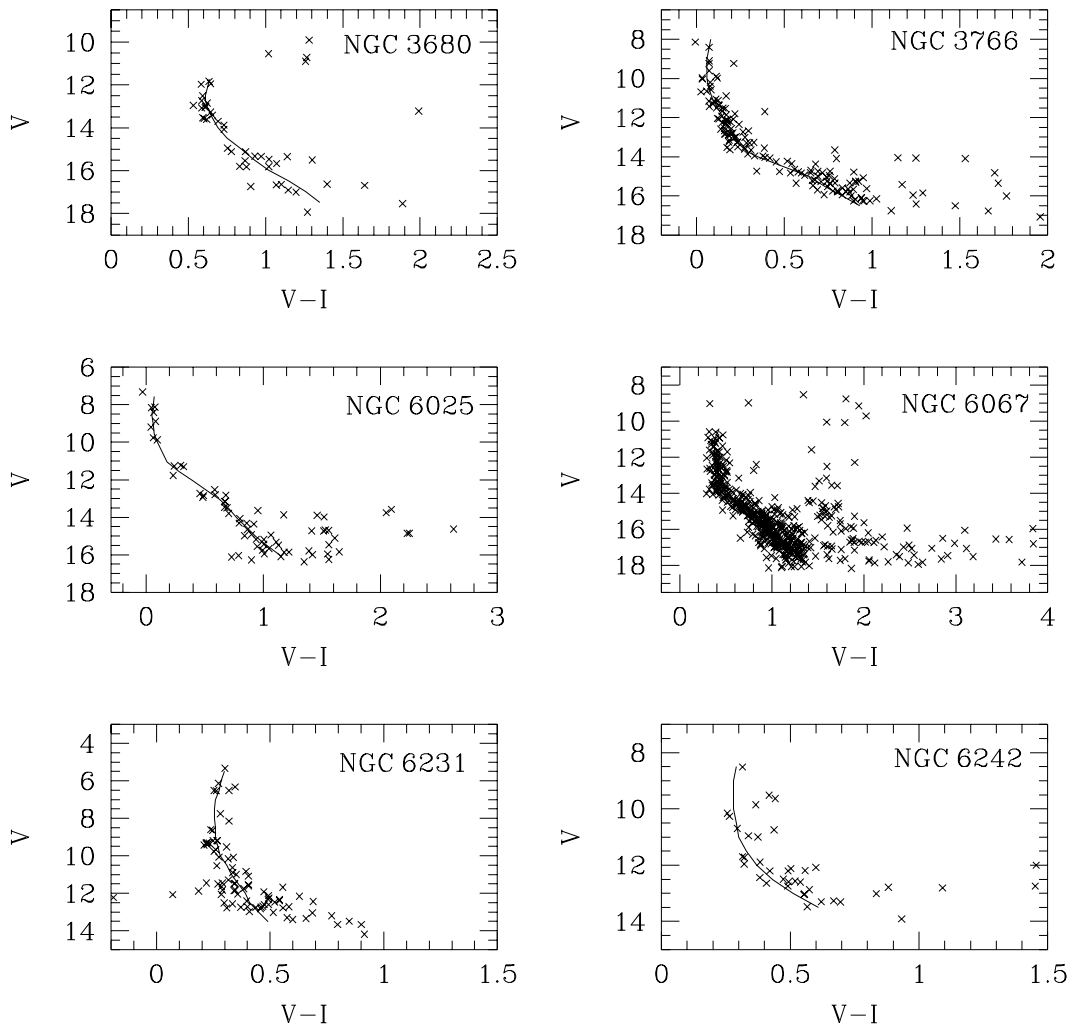


FIG. 1a

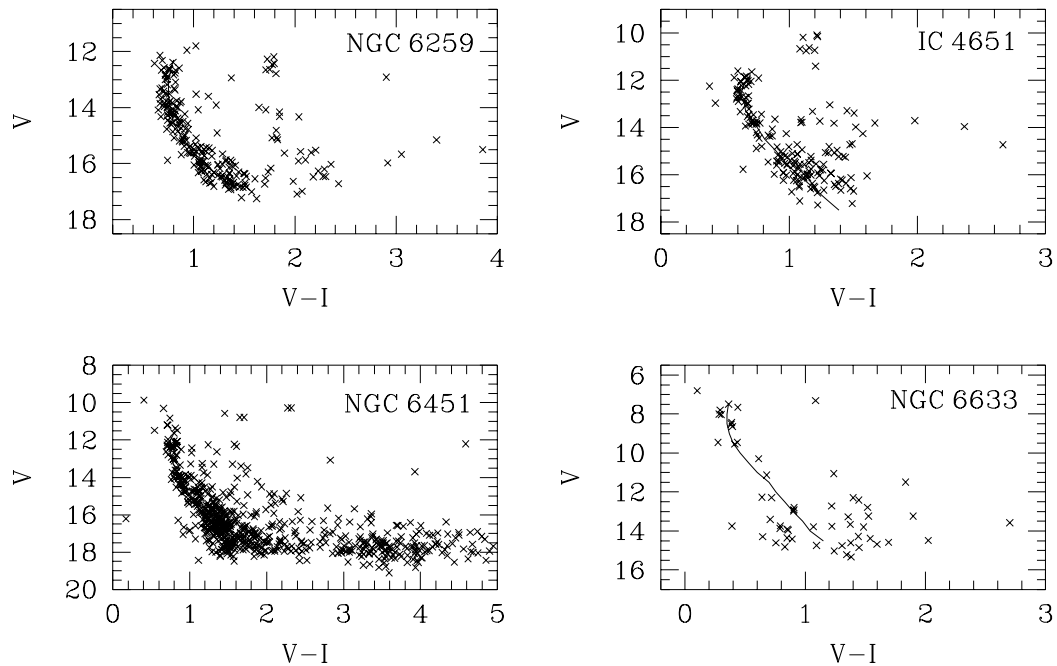


FIG. 1b

FIG. 1.—*C-M* diagrams of all template open clusters. Fiducial sequences are represented by solid lines. (a) NGC 3680, NGC 3766, NGC 6025, NGC 6067, NGC 6231, and NGC 6242; (b) NGC 6259, IC 4651, NGC 6451, and NGC 6633.

TABLE 14  
FUNDAMENTAL PARAMETERS FOR THE TEMPLATE OPEN CLUSTERS

Cluster	$E(B - V)$	References	$V - M_v$	References	Age (Myr)	References	[Fe/H]	References
NGC 3680.....	0.05	1, 2, 3	9.90	1, 2, 3, 4	1900	3, 4, 5	-0.16	6
NGC 3766.....	0.19	7, 8	11.85	9, 10	22	8	0.05	11
NGC 6025.....	0.17	12, 13	9.90	12, 13	110	12, 13	0.23	14
NGC 6067.....	0.33	12, 15	12.00	14, 15	160	12	0.00	6, 16
NGC 6231.....	0.45	12, 17, 18	12.60	12, 17, 18	5	12, 17, 19		
NGC 6242.....	0.39	8, 12, 20	11.45	8, 12, 20	50	8, 12	0.01	11
NGC 6259.....	0.66	22, 23	13.40	22, 23	200	12, 22	0.01	6
IC 4651.....	0.10	3, 12, 23, 24	10.00	12, 23, 25	2000	3, 12, 26	0.08	6
NGC 6451.....	0.08	14, 27	9.00	14, 27	4000	14, 27		
NGC 6633.....	0.17	28, 29	8.10	28, 29	630	14	-0.02	6

REFERENCES.—(1) Anthony-Twarog, Twarog, & Shodhan 1989b; (2) Anthony-Twarog et al. 1991; (3) Carraro & Chiosi 1994; (4) Mermilliod et al. 1995; (5) Carraro et al. 1993; (6) Piatti et al. 1995; (7) Mermilliod & Maeder 1986; (8) Battinelli & Capuzzo-Dolcetta 1991; (9) Shobbrook 1985; (10) Shobbrook 1987; (11) Luck & Bond 1989; (12) Meynet et al. 1993; (13) Feinstein 1971; (14) Lyngå 1987; (15) Walker 1985b; (16) Luck 1994; (17) Balona & Laney 1995; (18) Perry, Hill, & Christoudou 1991; (19) Santos & Bica 1993; (20) Moffat & Vogt 1973; (21) Anthony-Twarog, Payne, & Twarog 1989a; (22) Hawarden 1974; (23) Anthony-Twarog & Twarog 1987; (24) Smith 1982; (25) Kjeldsen & Frandsen 1991; (26) Anthony-Twarog et al. 1988; (27) Svolopoulos 1966; (28) Hiltner et al. 1958; (29) Schmidt 1976.

determination of interstellar reddening and distance from theoretical isochrones is reasonably accurate because these parameters are derived from the fitting of the ZAMS, which is satisfactorily reproduced by the theory (see, e.g., Mermilliod & Maeder 1986). The age determinations from theoretical isochrones, however, are somewhat more uncertain as they depend not only on the stellar evolutionary models (see, e.g., Twarog & Anthony-Twarog 1993, 1995) but also on the quality of the  $C-M$  diagrams. The morphology of the  $C-M$  diagram also plays a key role in this matter. Young open clusters, for example, have almost vertical MSs, which are difficult to fit (see, e.g., Bhatt et al. 1994; Sagar & Cannon 1994; Vázquez et al. 1995), while clusters several billion years old present subgiant and/or giant branches which can be reasonably well fitted by theoretical isochrones differing by 1 or 2 Gyr (see, e.g., Mazur et al.

TABLE 15  
NORMAL POINTS OF THE ZAMS

$M_v$	$(V - I)_0$	$M_v$	$(V - I)_0$
-3.5.....	-0.30	3.0.....	0.36
-3.0.....	-0.29	3.5.....	0.49
-2.5.....	-0.28	4.0.....	0.56
-2.0.....	-0.25	4.5.....	0.65
-1.5.....	-0.23	5.0.....	0.76
-1.0.....	-0.20	5.5.....	0.83
-0.5.....	-0.17	6.0.....	0.91
0.0.....	-0.15	6.5.....	1.05
0.5.....	-0.11	7.0.....	1.17
1.0.....	-0.06	7.5.....	1.30
1.5.....	0.02	8.0.....	1.45
2.0.....	0.09	8.5.....	1.60
2.5.....	0.21	9.0.....	1.75

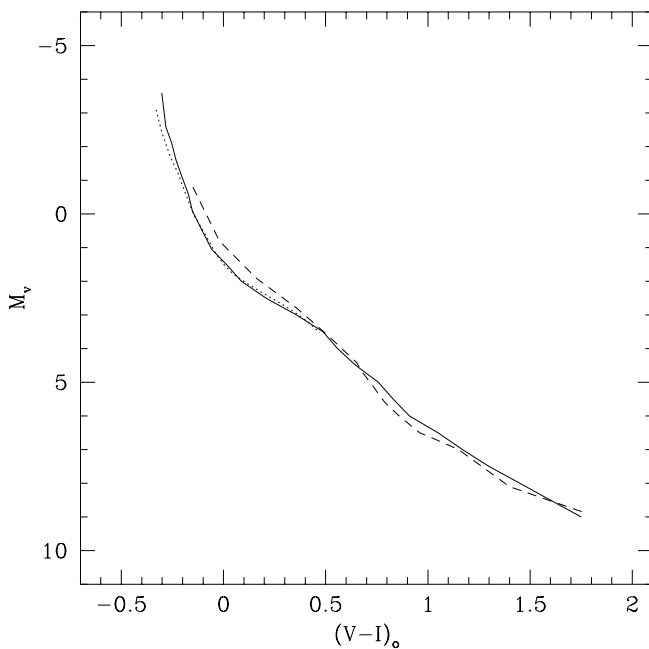


FIG. 2.—Zero-age main sequence (ZAMS) drawn from the 10 fiducial template clusters sequences (solid line). Walker's (1985a) (dotted line) and Straizys's (1990) (dashed line) ZAMS are also shown.

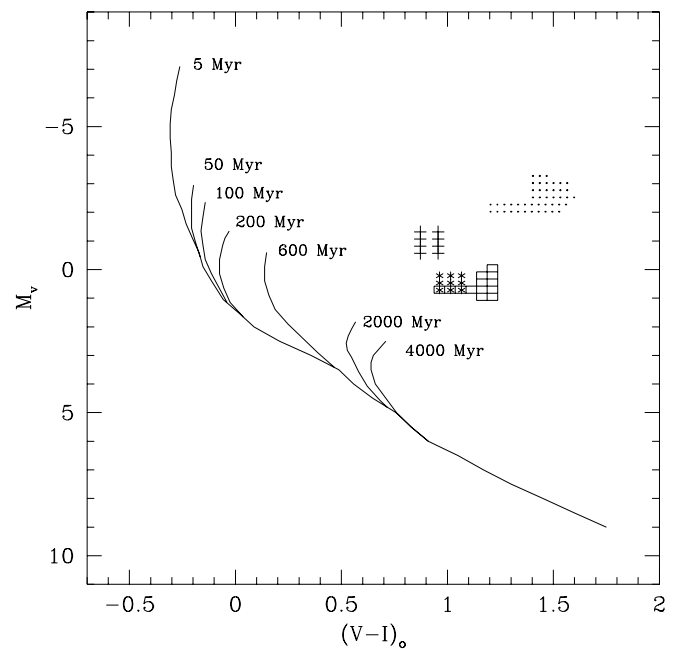


FIG. 3.—Composite  $M_v$  vs.  $(V - I)_0$  diagram calibrated in terms of age. Giant clump symbols: NGC 3680 (1900 Myr, squares); NGC 6067 (160 Myr, dots); NGC 6259 (200 Myr, plus signs); IC 4651 (2000 Myr, asterisks).

TABLE 16  
NORMAL POINTS IN THE  $M_v$  VERSUS  $(V-I)_0$  ISOCHRONOUS CURVES

$M_v$	$(V-I)_0$						
	5 Myr	50 Myr	100 Myr	200 Myr	600 Myr	2000 Myr	4000 Myr
-7.0.....	-0.26						
-6.5.....	-0.28						
-6.0.....	-0.29						
-5.5.....	-0.30						
-5.0.....	-0.31						
-4.5.....	-0.31						
-4.0.....	-0.30						
-3.0.....		-0.20					
-2.5.....		-0.21	-0.14				
-2.0.....		-0.21	-0.15				
-1.5.....		-0.21	-0.16	-0.03			
-1.0.....		-0.19	-0.15	-0.05			
-0.5.....		-0.17	-0.15	-0.06	0.15		
0.0.....			-0.12	-0.08	0.14		
0.5.....			-0.08	-0.07	0.14		
1.0.....			-0.05	-0.04	0.16		
1.5.....				0.0	0.19	0.57	
2.0.....				0.06	0.25	0.55	
2.5.....					0.32	0.52	0.71
3.0.....					0.39	0.55	0.65
3.5.....					0.47	0.58	0.64
4.0.....						0.62	0.66
4.5.....						0.68	0.71
5.0.....							0.76
5.5.....							0.83
6.0.....							0.91

1993; Kassis, Friel, & Phelps 1996). Furthermore, when the cluster metallicity is unknown, as is the case of most of the faint open clusters recently studied, the age determination has an additional source of uncertainty. In fact, isochrones corresponding to a range of different ages and metallicities can fit the observed  $C-M$  diagram of an open cluster reasonably well. However, the changes in the morphology of the isochrones owing to metallicity variations depend on the considered color index. These changes are negligible if  $(V-I)_0$  is used instead of  $(B-V)_0$ , since the former index is virtually free from metallicity effects for open clusters (Rosvick 1995). Recently, Kassis et al. (1996) appropriately fitted isochrones of 5 Gyr with  $[\text{Fe}/\text{H}] = -0.23, -0.45$  and  $-0.75$  to the observed  $V$  versus  $V-I$  diagram of the open cluster ESO 092-SC18 by simultaneously varying other parameters such as distance and reddening. The theoretical models have been successively modified and improved according to the constraints placed by the increasing quantity and quality of observational data. At present, classical models computed from canonical precepts (e.g., Castellani, Chieffi, & Straniero 1992) may be distinguished from those including overshooting effects (e.g., Schaller et al. 1992). Among the most popular models, only those obtained by Vandenberg (1985; hereafter VB) and Bertelli et al. (1994; hereafter BBCFN) have isochrones computed for the  $(M_v, [V-I]_0)$  plane. The isochrones of BBCFN range between 5 Myr and 16 Gyr. They take into account overshooting effects and describe the loops of the red giant phase, as well as the white dwarf phase. The isochrones of VB do not include convective overshooting mixing and cover only the intermediate-age and old open cluster age range. With the purpose of examining the performance of the theoretical isochrones, we have compared those derived by VB and BBCFN with the empirical ones obtained in § 3. Since we have calibrated the  $M_v$  versus  $(V-I)_0$  plane in terms of age

using template clusters with typically solar metal content, only theoretical isochrones corresponding to  $Z \approx 0.02$  have been selected. A total of three of VB's isochrones ( $t = 0.6, 2.0,$  and  $4.0$  Gyr) extending up to the subgiant stage and seven BBCFN's isochrones ( $\log t = 6.6, 7.7, 8.0, 8.3, 8.8, 9.3,$  and  $9.6$ ) were compared to the empirical isochrones of Figure 3, from the ZAMS to the red giant loop. Figure 4 shows the isochrones of VB (*dotted lines*) compared to those

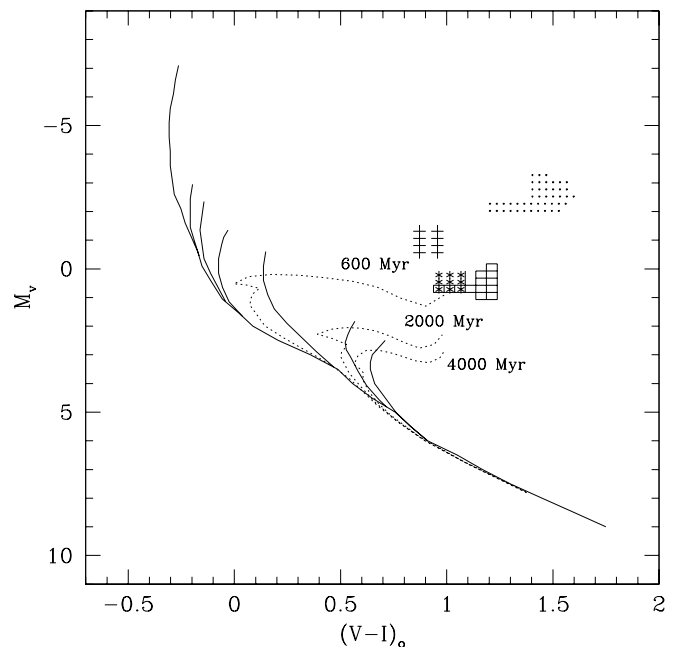


FIG. 4.—Comparison between Fig. 2 and Vandenberg's (1985) isochrones (*dotted lines*) for clusters with ages of 0.6, 2, and 4 Gyr.

obtained in the present work (*solid lines*). The following conclusions may be drawn from a simple inspection of Figure 4: (1) Both ZAMSs show a very good agreement within the common absolute magnitude range. The only noticeable difference appears at  $M_v \sim 5$  ( $\Delta M_v \approx 0.25$  mag), where the evolved MS of NGC 6451 (4 Gyr isochrone) begins. (2) The theoretical and empirical turnoff points show a generally good agreement, although the former ones appear to be systematically bluer and fainter. These discrepancies are more appreciable for the 0.6 Gyr isochrone of VB. Notice that the empirical 0.6 Gyr isochrone corresponding to NGC 6633 also presents an excess of bright MS stars at  $M_v \sim -0.5$  mag. A comparison of the empirical isochrones of Figure 3 (*solid lines*) with the theoretical ones of BBCFN (*dotted lines*) is shown in Figure 5. Both sets of isochrones show an overall very good agreement. As can be seen, the empirical ZAMS reproduces the theoretical one satisfactorily throughout the entire range of absolute magnitudes. The ZAMSs appear to be slightly different ( $\Delta M_v \leq 0.2$  mag) only at  $M_v \sim 3$ , where the theoretical ZAMS describes a slightly more pronounced curvature. Notice that the difference observed with the ZAMS of VB at  $M_v \sim 5$  (see Fig. 4) is now negligible. Notice also that, even though the isochrones of VB and BBCFN were computed using different  $Y$  values ( $Y_{VB} = 0.25$ ;  $Y_{BBCFN} = 0.28$ ), the corresponding ZAMS appears to be appropriately placed. Therefore, the small differences among the theoretical and empirical isochrones probably arise from differences in the input physics and the evolutionary codes used. The turnoffs of BBCFN and the empirical ones show very good agreement in general, although small differences are evident in Figure 5. For the 50 and 100 Myr isochrones, the empirical turnoffs are slightly bluer than the theoretical ones. In the case of the 50 Myr isochrone, the small difference very likely arises from the fact that the empirical isochrones were defined by averaging the fiducial sequences of NGC 3766 and NGC 6242, despite the fact that the former cluster is

only 22 Myr old. Thus, the empirical 50 Myr isochrone actually represents the MS of a cluster somewhat younger than 50 Myr. The almost vertical position of young open clusters MSs also makes it difficult to estimate their ages. NGC 6025 should be 70 Myr old according to BBCFN, instead of 110 Myr adopted in the present calibration. For  $\log t = 8.8, 9.3$ , and  $9.6$ , the isochrones of BBCFN improve the fits of the empirical turnoffs as compared to those of the isochrones of VB. However, the excess of bright MS stars in NGC 6633 (600 Myr isochrone) is still noticeable. Finally, the comparison between the turnoffs of NGC 6231 (5 Myr) and NGC 6067 (200 Myr) with the isochrones of  $\log t = 6.6$  and  $8.3$ , respectively, presents an excellent agreement. As shown in Figure 5, a comparison of the observed red giant clumps with the theoretical stellar evolutionary paths reveals, in general, that the theoretically computed bluest stages during the He-burning core phase are redder than the observed colors of the cluster red giants in IC 4651 and NGC 6259. This is not the case for the observed giants in NGC 6067 that lie at the tip of the 200 Myr red giant phase. A similar result was found by Meynet, Mermilliod, & Maeder (1993) from the fitting of isochrones in the  $M_v$  versus  $(B-V)_0$  diagram. All clusters older than 200 Myr have observed giant clumps bluer than the loops computed by Schaller et al. (1992), except NGC 6067 whose giants are spread out over redder  $(B-V)_0$  colors. Other independent earlier analyses also suggest the existence of a shift between the observed loops and theoretical ones for clusters older than 200 Myr (see, e.g., Clariá et al. 1994; Rosvick 1995).

## 5. CONCLUSIONS

We have obtained CCD photometric data using the  $VI$  Johnson-Cousins filters for a total of 10 template open clusters with accurately known fundamental parameters. These clusters were carefully chosen to calibrate the  $M_v$  versus  $(V-I)_0$  diagram in terms of age. The photometric data allowed us to construct well-defined  $C-M$  diagrams. Once the fiducial sequences were traced in the  $V$  versus  $V-I$  diagrams, we performed the transformation into the  $M_v$  versus  $(V-I)_0$  plane and averaged sequences of template clusters with nearly similar age. The empirical ZAMS in the resulting composite  $M_v$  versus  $(V-I)_0$  diagram agrees very well with those previously obtained by Walker (1985a) and Straizys (1990) over a wide range of absolute magnitudes. A homogeneous set of empirical isochrones in the  $M_v$  versus  $(V-I)_0$  plane was obtained for clusters with ages between 5 Myr and 4 Gyr. This age range represents an important fraction of the time interval during which the chemical evolution of the Galactic disk has occurred. The present calibration of the  $M_v$  versus  $(V-I)_0$  diagram as a function of age should be very useful in determining reddening, distance, and age of unstudied open clusters located in obscured regions of the Milky Way. A comparison between the empirical isochrones obtained in the  $M_v$  versus  $(V-I)_0$  plane with those computed from stellar evolutionary models by VB and BBCFN show an overall very good agreement. The empirical ZAMS is well fitted by both canonical and non canonical theoretical models. The isochrones of BBCFN noticeably improve the fit of the turnoff points with respect to the isochrones of VB for clusters older than 600 Myr. Finally, the observed red giant clumps in the  $M_v$  versus  $(V-I)_0$  plane are found to be slightly bluer than the theoretical loops of BBCFN. We are grateful to the

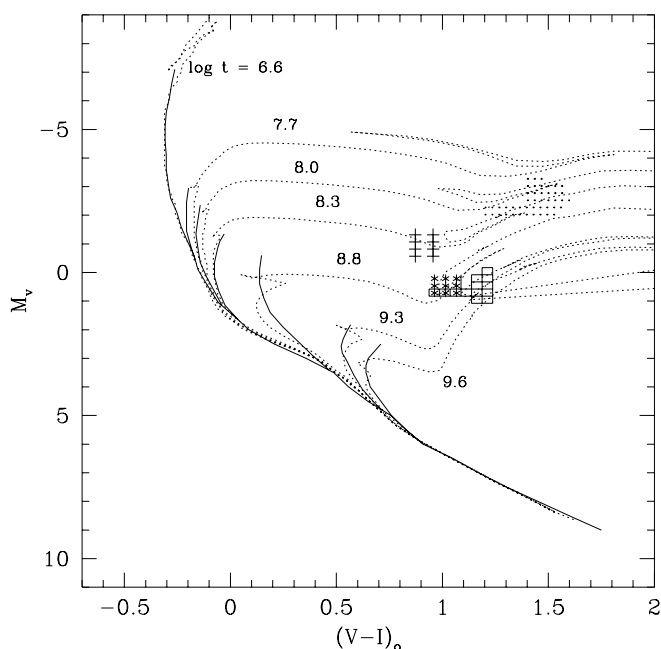


FIG. 5.—Comparison between Fig. 2 and Bertelli et al.'s (1994) isochrones (*dotted lines*).

staff at Las Campanas Observatory for their kind hospitality and assistance during the observing run.

We also thank D. Geisler for reading the manuscript and

helpful suggestions. This work was partially supported by the institutions CONICET and CONICOR (Argentina) and CNPq and FINEP (Brazil). We also acknowledge support from the Vitae and Antorchas foundations.

## REFERENCES

- Alter, G., Ruprecht, J., & Vanýsek, J. 1970, *Catalogue of Star Clusters and Associations*, ed. G. Alter, B. Balázs, & J. Ruprecht (Budapest: Akademiai Kiado)
- Anthony-Twarog, B. J., Heim, E. A., Twarog, B. A., & Caldwell, N. 1991, *AJ*, 102, 1056
- Anthony-Twarog, B. J., Mukherjee, K., Twarog, B. A., & Caldwell, N. 1988, *AJ*, 95, 1453
- Anthony-Twarog, B. J., Payne, D. M., & Twarog, B. A. 1989a, *AJ*, 97, 1048
- Anthony-Twarog, B. J., & Twarog, B. A. 1987, *AJ*, 94, 1222
- Anthony-Twarog, B. J., Twarog, B. A., & Shodhan, S. 1989b, *AJ*, 98, 1634
- Balona, L. A., & Laney, C. D. 1995, *MNRAS*, 276, 627
- Battinelli, P., & Capuzzo-Dolcetta, R. 1991, *MNRAS*, 249, 76
- Bertelli, G., Bressan, A., Chiosi, C., Fagotto, F., & Nasi, E. 1994, *A&AS*, 106, 275 (BBFCN)
- Bhatt, B. C., Pandey, A. K., Mahra, H. S., & Paliwal, D. C. 1994, *Bull. Astron. Soc. India*, 22, 291
- Carraro, G., Bertelli, G., Bressan, A., & Chiosi, C. 1993, *A&AS*, 101, 381
- Carraro, G., & Chiosi, C. 1994, *A&A*, 287, 761
- Carraro, G., & Ortolani, S. 1994, *A&A*, 291, 106
- Castellani, V., Chieffi, A., & Straniero, O. 1992, *ApJS*, 78, 517
- Clariá, J. J., Mermilliod, J. C., Piatti, A. E., & Minniti, D. 1994, *A&AS*, 107, 39
- Daniel, S. A., Latham, D. W., Mathieu, R. D., & Twarog, B. A. 1994, *PASP*, 106, 281
- Feinstein, A. 1971, *PASP*, 83, 800
- Friel, E. D., & Janes, K. A. 1993, *A&A*, 267, 75
- Geisler, D., Clariá, J. J., & Minniti, D. 1992, *AJ*, 104, 1892
- Hawarden, T. G., 1974, *MNRAS*, 169, 539
- Hiltner, W. A., Iriarte, B., Johnson, H. L. 1958, *ApJ*, 127, 539
- Kassis, M., Friel, E. D., & Phelps, R. L. 1996, *AJ*, 111, 820
- Kjeldsen, H., & Frandsen, S. 1991, *A&AS*, 87, 119
- Kozhurina-Platais, V., Girard, T. M., Platais, I., van Altena, W. F., Ianna, Ph. A., & Cannon, R. D. 1995, *AJ*, 109, 672
- Landolt, A. U. 1983, *AJ*, 88, 439
- . 1992, *AJ*, 104, 340
- Luck, R. E. 1994, *ApJS*, 91, 309
- Luck, R. E., & Bond, H. E. 1989, *ApJS*, 71, 559
- Lyngå, G. 1987, *Catalogue of Open Clusters* (Strasbourg: Centre de Données Stellaires)
- Mazur, B., Kaluzny, J., & Krzemiński, W. 1993, *MNRAS*, 265, 405
- Mermilliod, J. C. 1981a, *A&AS*, 44, 467
- . 1981b, *A&A*, 97, 235
- Mermilliod, J. C., Andersen, J., Nordström, B., & Mayor, M. 1995, *A&A*, 299, 53
- Mermilliod, J. C., & Maeder, A. 1986, *A&A*, 158, 45
- Mermilliod, J. C., Mayor, M., & Burki, G. 1987, *A&AS*, 70, 389
- Meynet, G., Mermilliod, J. C., & Maeder, A. 1993, *A&AS*, 98, 477
- Moffat, A. F. J., & Vogt, N. 1973, *A&AS*, 10, 135
- Montgomery, K. A., Marschall, L. A., & Janes, K. A. 1993, *AJ*, 106, 181
- Nordström, B., Andersen, J., & Andersen, M. I. 1996, *A&AS*, 118, 407
- Patat, F., & Carraro, G. 1995, *MNRAS*, 272, 507
- Perry, C. L., Hill, G., & Christoudou, D. M. 1991, *A&AS*, 90, 195
- Piatti, A. E., Clariá, J. J., & Abadi, M. G. 1995, *AJ*, 110, 2813
- Rosvick, J. M. 1995, *MNRAS*, 277, 1379
- Sagar, R., & Cannon, R. D. 1994, *Bull. Astron. Soc. India*, 22, 381
- . 1995, *A&AS*, 111, 75
- Sanders, W. L. 1973, *A&AS*, 9, 213
- Santos, J. F. C., & Bica, E. 1993, *MNRAS*, 260, 915
- Schaller, G., Schaerer, D., Meynet, G., & Maeder, A. 1992, *A&AS*, 96, 269
- Schmidt, E. G. 1976, *PASP*, 88, 63
- Shobbrook, R. R. 1985, *MNRAS*, 212, 591
- . 1987, *MNRAS*, 225, 999
- Smith, G. H. 1982, *AJ*, 87, 360
- Stetson, P. B. 1991, *DAOPHOT User Manual*
- Straizys, V. 1990, *Multicolor Stellar Photometry* (Tucson: Pachart)
- Svolopoulos, S. N. 1966, *Z. Astrophys.*, 64, 67
- Twarog, J. C., & Anthony-Twarog, B. J. 1993, *PASP*, 105, 78
- . 1995, *PASP*, 107, 1215
- VandenBerg, D. A. 1985, *ApJS*, 58, 711 (VB)
- Vázquez, R. A., Will, J. M., Prado, P., & Feinstein, A. 1995, *A&AS*, 111, 85
- Walker, A. R. 1985a, *MNRAS*, 213, 889
- . 1985b, *MNRAS*, 214, 45